Stochastic Environmental Research and Risk Assessment (2023) 37:2513–2540
https://doi.org/10.1007/s00477-023-02403-6

ORIGINAL PAPER

# Proposing an ensemble machine learning based drought vulnerability index using M5P, dagging, random sub-space and rotation forest models

Sunil Saha[1] · Barnali Kundu[1] · Gopal Chandra Paul[1] · Biswajeet Pradhan[2,3]

Accepted: 11 February 2023 / Published online: 6 March 2023


**Abstract**
Drought is one of the major barriers to the socio-economic development of a region. To manage and reduce the impact of drought, drought vulnerability modelling is important. The use of an ensemble machine learning technique i.e. M5P, M5P - Dagging, M5P-Random SubSpace (RSS) and M5P-rotation forest (RTF) to assess the drought vulnerability maps (DVMs) for the state of Odisha in India was proposed for the first time. A total of 248 drought-prone villages (samples) and 53 drought vulnerability indicators (DVIs) under exposure (28), sensitivity (15) and adaptive capacity (10) were used to produce the DVMs. Out of the total samples, 70% were used for training the models and 30% were used for validating the models. Finally, the DVMs were authenticated by the area under curve (AUC) of receiver operating characteristics, precision, mean-absolute-error, root-mean-square-error, K-index and Friedman and Wilcoxon rank test. Nearly 37.9% of the research region exhibited a very high to high vulnerability to drought. All the models had the capability to model the drought vulnerability. As per the Friedman and Wilcoxon rank test, significant differences occurred among the output of the ensemble models. The accuracy of the M5P base classifier improved after ensemble with RSS and RTF meta classifiers but reduced with Dagging. According to the validation statistics, M5P-RFT model achieved the highest accuracy in modelling the drought vulnerability with an AUC of 0.901. The prepared model would help planners and decision-makers to formulate strategies for reducing the damage of drought.

**Keywords** Drought vulnerability · Ensemble machine learning model · Exposure index · Sensitivity index · Adaptive capacity index · GIS

## 1 Introduction

Drought vulnerability assessment is becoming an important topic of research due to the increased interest in developing evaluation approaches and adaptation strategies that are associated with climate change. Frequent droughts and tremendous heat events, according to the Intergovernmental Panel on Climate Change (IPCC, 2001), might increase drought vulnerability and effects on socio-economic condition of the region. Drought, an inherent feature of the earth's climate, frequently emerges without notice and with no discernible borders, resulting in yearly agriculture damage that costs billions of dollars (Ortiz-Bobea 2021). Drought impacts nearly all climatic zones (Ajayi & Ilori 2020) and over half of the world every year (Feng et al. 2019a, b). According to Rosselló et al. (2020), drought ranks first among natural catastrophes in terms of the number of people directly impacted across the world. Drought happens in high- and low-rainfall locations and in all climatic zones; its repercussions are crucial and costly, impacting more people globally than other natural catastrophes (Mishra et al. 2021). Drought has varying consequences based on the degree of progress and coping skills of regions and nations; it affects the economy and livelihood, as well as the trade of public and private companies in developing nations.

Other significant catastrophes, such as cyclones, floods and droughts, affect the economy of India. Drought occurs on a regular basis in various parts of the country. Drought is a geographically widespread hazard globally. As per the recent study by the National Centre for Atmospheric Research (NCAR), the percentage of severe drought

Extended author information available on the last page of the article

affected area has increased four times in the Earth since 1970 to the 2000. According to Baarsch et al. (2020), the percentage of worldwide land experiencing very dry circumstances increased from 10 to 15% in 1970s to over 30% in 2002. Drought vulnerability is receiving more attention because of its significant economic consequences and social risk concerns (Karimi et al. 2018; Haile et al. 2020). Drought vulnerability depends on the water resources system's dependability and capacity to adapt efficiently, and it may increase with population growth, with different water requirements, and with the intensification of the conflicting demands for water resources (Thomas et al. 2016; Hoque et al. 2021). In disaster management, drought vulnerability assessment is the latest paradigm that helps decision makers plan for drought, assign resources and mitigate damage. The degree of drought exposure and the area's damage coping capabilities determine a region's vulnerability to drought, and underdeveloped places with weaker coping capacities and greater exposure are at the greatest danger. Vulnerability of any area is determined by exposure, sensitivity and adaptive capacity (Intergovernmental Panel on Climate Change [IPCC] 2001). While sensitivity refers to how much a system is affected by a disaster, adaptive capacity refers to how well a system can withstand and absorb a disaster, and exposure refers to how much and how long a population is exposed to a disaster (Ebi et al. 2006).

Vulnerability includes both temporal and spatial aspects, because it evolves in response to technological changes, human behaviour, activities and legislation (Bevacqua et al. 2018; Turner 2021). The vulnerability manifests itself in certain places at various times, indicating that it is context-, place- and time-specific, as well as particular to the viewpoint of the individual judging it (Germain and Knight 2021). In the fields of geography, agricultural science, water resources, climate science and social science, numerous studies on assessment of vulnerability have been conducted (Mukherjee et al. 2019). Some scholars have established quantitative methods of drought vulnerability (Han and Zhang 2018; Hurlbert and Gupta 2019; Sharafi et al. 2020), whereas others have tried to conceptualise the character of vulnerability from different theoretical perspectives (Kaufman et al. 2020).

Creating techniques for measuring vulnerability is challenging because of the difficulty of the systems under investigation and the premise that susceptibility is not an immediately detectable phenomenon (Alodah 2019; Datta 2019). A rigorous assessment of vulnerability is critical, because it may help build focused drought prevention and response plans. Murthy (2020) devised a statistical weighting methodology to measure the potential of agricultural drought and found that non-irrigated farmland and ranging land on sandy soils seem to be the places most sensitive to agricultural drought. The security graph idea was utilised by West et al. (2019) to measure the susceptibility to dryness of India under extreme climatic stress; environmental pressure was obtained from indications of water stress created by the model of Water Gap. The World Meteorological Organization (WMO) suggested the use of the standardised precipitation index (SPI) (Kobrossi et al. 2021) as the worldwide index to assess drought. Nyairo et al. (2020) used dynamic system analytic methods to explore the vulnerability of the food system to climate change and the degradation of land in the pastoral area of Kalahari of Botswana with emphasis on drought susceptibility. Huynh and Stringer (2018) offered an outline of the susceptibility to climatic change of the connected systems of social ecology. Guo et al. (2021) evaluated the drought vulnerability across three intensities of drought, namely, very-high, extremely-high and critical regions, for the farmers who produce wheat in the western part of Iran. They concluded that drought vulnerability influences the socio-cultural and economic conditions. Banihashemi et al. (2021) established and assessed drought susceptibility parameters among the farmers who produce wheat in Mashhad County, Iran, including social, economic and technical variables. Paul et al. (2020) used multi-attribute strategic planning techniques depending on a set of criteria, performance and various indicators to build a novel extremely effective technique for geographical evaluation of drought susceptibility in Iran for the river basin of Zayandeh-Rood. Thomas et al. (2016) created a drought vulnerability indicator (DVI) that depicts multiple dimensions of drought susceptibility assessed at the Pan African level depending on economic capability, renewable natural capital, societal and human resources, technology and infrastructure.

The present research was conducted in the state of Odisha, India, where drought is a serious concern (Senapati 2019; Saha et al 2021). A large part of Odisha is frequently affected by drought (Sahu and Nandi 2016). Farmers in the state are frequently affected by drought, which leads to many agricultural losses. Numerous works have been done to predict or forecast drought conditions throughout the world in consideration of different machine learning techniques. Methods such as artificial neural network (Nabipour et al. 2020), random forest (Dikshit et al. 2020) and support vector machine (Zahraie and Nasseri 2011) for hydrological and meteorological drought forecasting provided good results. When Dikshit et al. (2021a; 2021b) employed a variety of deep learning algorithms to anticipate drought, the results were superior to those produced using conventional statistical methods.

Utilizing conventional statistical techniques, some research have been done on assessing drought vulnerability. Recently, Hoque et al. (2020; 2021) and Saha et al

(2021) used analytical hierarchical process (AHP) and Fuzzy-AHP methods to analyse drought vulnerability. Saha et al. (2021a) used ANN and Bagging method for assessing the drought vulnerability situation of Karnataka state. In order to model the susceptibility of various hazards, a variety of ensemble machine learning algorithms (MLAs) were utilised, including landslide (Antronico et al. 2020), gully erosion (Roy et al. 2021), land subsidence (Tien Bui et al. 2018), deforestation (Saha et al. 2021b) and flood (Nhu et al. 2020a, b, c), rather than drought. Better accuracy was obtained compared with when conventional statistical and semi-quantitative methods were used (Dikshit et al. 2020). Combining various models is advised in order to decrease model mistakes and improve forecast accuracy. Although each combination demonstrated greater modelling prediction performance with high dependability, new ensemble-based techniques still need to be investigated and used. In various geo-hazards, ensemble models including bagging, boosting, and stacking have frequently been used. By building a number of prediction functions and then combining them in a certain way to create a predictive function, bagging helps to enhance unstable estimating or classification schemes and may be used to increase the accuracy of learning algorithms. Boosting has the ability to correct the poor classifier mistakes made by unreliable learners. Its core concept is to train several weak classifiers on the same training set, then combine these weak classifiers to create a stronger final classifier (Freund and Schapire 1997). A learning algorithm is taught to aggregate the predictions of multiple different learning models in a technique called stacking, which is an ensemble learning approach that often produces greater performance than any trained model alone (Wolpert 1992). It is important to keep in mind that models with theoretically ideal performance may not always produce superior outcomes in practical situations. Furthermore, it is uncertain if different ML techniques may be applied or generalized in varied geographic situations.Most of the MLAs were used for forecasting the drought conditions rather than drought vulnerability. Dagging, Random Subspace (RSS), and Rotation Forest (RTF) were applied in landslide, flood and deforestation susceptibility modelling (Pham et al. 2017; Wang et al. 2020; Saha et al 2021b) except drought vulnerability modelling and provided good results. The main research questions are as follows: (1) can ensemble MLAs provide better results than the conventional statistical and semi-quantitative methods in drought vulnerability assessment? (2) can meta classifiers increase the level of accuracy of base classifier (M5P) in drought vulnerability modelling? Therefore, the main novelty of our work is the assessment of the drought vulnerability of Odisha using ensemble models, such as M5P, M5P-Dagging, M5P-RSS and M5P-RTF. To conduct this research, a wide variety of exposure, sensitivity and adaptive capacity (total 53 factors) were used to account for all possible drought scenarios. The criteria were chosen according to past research, and the evaluation was conducted using well-known MLAs. In each case, the capacity for forecasting of the output of the model was enormously appreciable. As a result, using MLAs is nothing new. The use of these ensemble machine learning models to evaluate drought vulnerability by taking into account as many as 53 parameters, however, is special. The primary goal of the current study is to develop a relative drought vulnerability map for Odisha using a variety of meteorological, hydrological and socioeconomic factors.

## 2 Materials and methods

### 2.1 Study area

Odisha is situated on India's eastern coast, which spans from 17.31°N to 22.31°N latitudes and 81.31° E to 87.29° E longitudes geographical coordinates (Fig. 1). The region's coastline stretches for 485 km all along the Bay of Bengal. High temperatures, heavy humidity, medium to high rainfall and brief and mild winters define Odisha's climate. A tropical climate defines the state (Santos et al. 2021). The state's average rainfall is 1451.2 mm, most of which falls between June and September. Drought, floods and cyclones occur every year, with various degrees of intensity (Pidathala et al. 2018). The central plateaus, Utkal plains, central mountains, western hills, highlands and floodplains and western hills and floodplains are the five primary physiographic zones of Odisha. Brahmani, Mahanadi and Baitarani are the state's main rivers, all of which flow into the Bay of Bengal. Odisha has a population of 42 million, according to the 2011 Indian Census (3.47% of the total population of India). Drought is not unknown to the people of Odisha, as it happens every year in several parts of the state, with variable degrees of intensity and scale. The first severe drought in the state occurred in 1866 (Saha et al 2021a). Since then, the state has experienced several moderate-to-severe drought events. This indicated that droughts of moderate-to-high intensity occur every 8 years or so in Odisha. Droughts of exceptional intensity occurred in Odisha in 1866, 1919, 1965, 2000–2001, 2015 (www.business-standard.com/article/current-affairs) and 2019 (Swain et al. 2021a, b). The 2000–2001 drought was

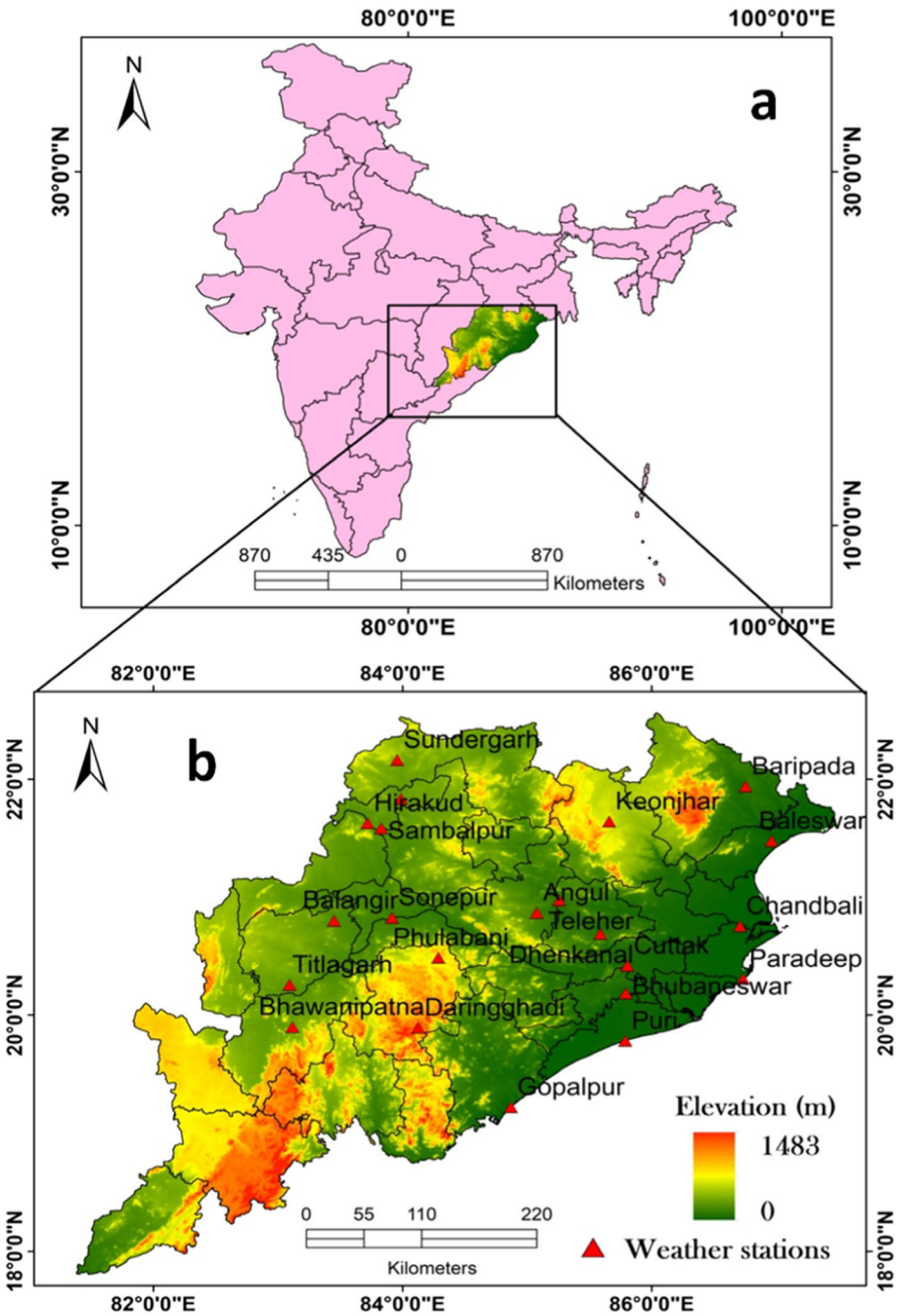


**Fig. 1** Location of the study area: a India, and b. Odisha showing the locations of weather stations

the most devastating. Droughts hit nine districts throughout Odisha in 2018, the most of which were in western Odisha, where farmers faced crop losses of 33% and higher owing to moisture stress. Drought hit at least 25 of the 30 districts in 2015, owing to an irregular southwest monsoon. Drought has long been a problem in the state's western and south-central regions. In terms of strategic management and planning, a drought risk analysis of this state is critical.

## 2.2 Methodology

The drought vulnerability maps were produced using four well-known MLAs in the following four phases (Fig. 2).

*Step-1*: **selection of vulnerability parameters:** The selection of the drought vulnerability factors (DVFs) was based on a review of the literatures and the state of the environment. The variables were then separated into three sub-categories, namely exposure, sensitivity, and adaptive capability.

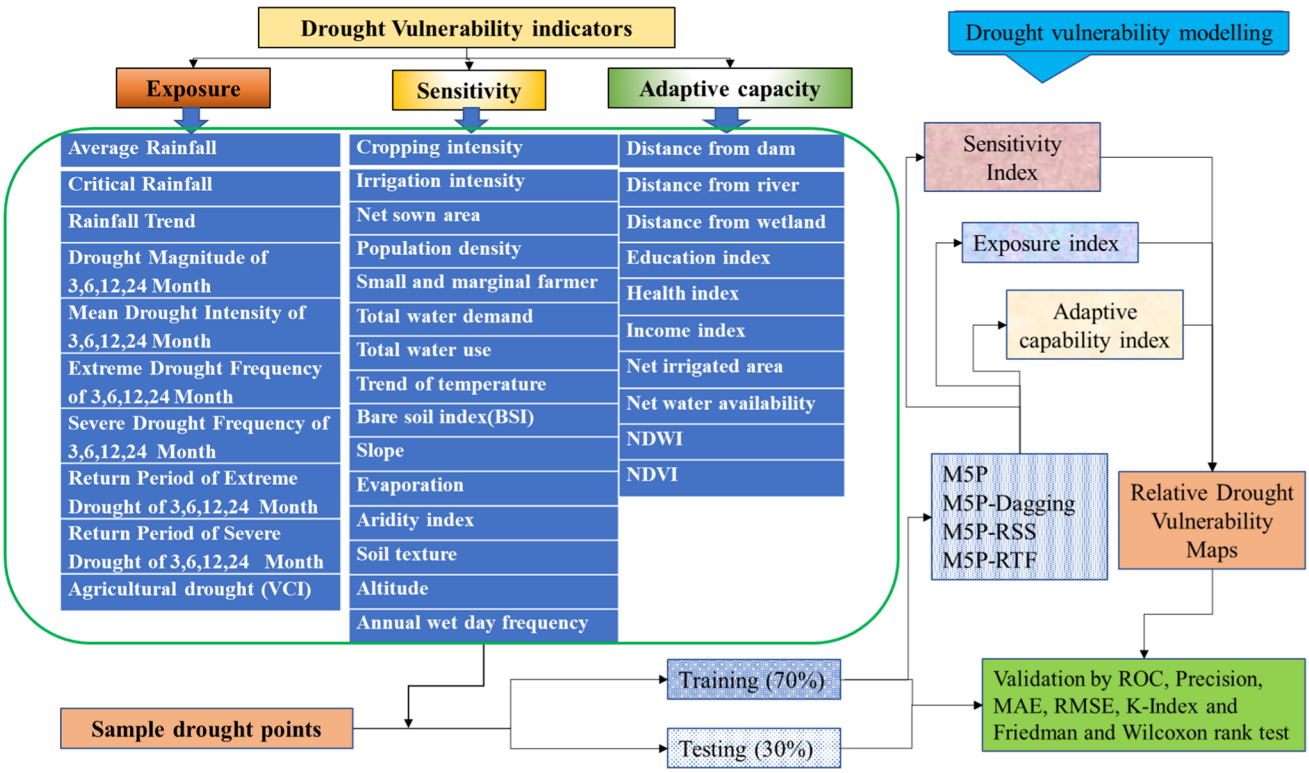


**Fig. 2** Methodological flow chart

*Step-2*: **Development of the thematic data layers:** To forecast spatial drought vulnerability, data on drought-impacted villages and DVFs were gathered.

*Step-3*: **DV maps preparation:** With the aid of training datasets, ensemble machine learning models (M5P, M5P-Dagging, M5P-RTF and M5P-RSS) were used to create drought vulnerability maps. Specific indices, such as exposure, sensitivity and adaptive capability, were assessed using a set of chosen parameters and to generate the final vulnerability map. Finally, three indices were used to create the vulnerability map of drought.

*Step-4*: **validation and comparison of the models:** To verify the used models, the AUC-ROC, precision, K-index, root mean square error (RMSE) and mean absolute error (MAE) were used. Friedman and Wilcoxon rank tests methods were also used to examine the dissimilarities in the models' prediction performance.

## 2.3 Constructing spatial data layers

Identification of current drought-impacted regions is critical for drought vulnerability mapping. A total of 248 drought affected areas (points) were collected from the Odisha state record and were divided into 70:30 ratio among testing and training points (Fig. 2). Similarly, same number of non-drought affected locations were selected randomly for training and testing the applied models. Both drought and non-drought locations were identified after consulting the data from the Disaster Management Department of Odisha and local dwellers. Various factor layers have been created in the ArcGIS environment based on the available data (Table 1). Various socioeconomic and meteorological characteristics (a total of 53 parameters) were chosen based on prior literature and geo-environmental condition of the study area (Table 2). These parameters were then divided into three categories, namely, adaptive ability, sensitivity and exposure. After taking into account all of the layers, data incorporation and analysis were completed. For producing the final drought vulnerability maps resolution of DEM (30 m*30 m) was considered as base resolution and the other factors having the resolution more or less than the DEM were resampled. Afterwards, the M5P model was utilised as a basis classifier, and three more models were used to create the novel ensemble models. M5P-Dagging, M5P-RSS and M5P-RTF were the ensemble models.

### 2.3.1 Exposure indicators

These variables indicated the degree to which a region or its people are subjected to drought (Table 3). Severe drought frequency (%) of 3, 6, 12 and 24 months,

**Table 1** Source of considered parameters

| Data | Sources | Time/ period |
|---|---|---|
| Rainfall | Indian Meteorological Department (IMD) | 1960–2019 |
| Landsat 8 | Earthexplore.usgs.gov | 2021 |
| Cropping intensity | District irrigation plan, Odisha | 2016 |
| Irrigation intensity | A study on Irrigation and Agricultural productivity in Odisha | 2018 |
| Net sown area | District irrigation plan, Odisha | 2016 |
| Population density | District irrigation plan, Odisha | 2016 |
| Small and marginal farmer | Odisha, Agriculture Statistics | 2013–2014 |
| Total water demand | Ground water booklet, Odisha | 2016 |
| Total water use | Ground water booklet, Odisha | 2016 |
| Temperature | Indian Meteorological Department (IMD) | 1960-2019 |
| Evaporation | Indian Meteorological Department (IMD) | 1960-2019 |
| Aridity index | https://cgiarcsi.community/2019/01/24/global-aridity-index-and-potential-evapotranspiration-climate-database-v2/ | 1970–2019 |
| Soil texture | https://www.slideshare.net/csisaproject/10-july-2012-directorate-of-agriculture-odisha | – |
| DEM | Earthexplore.usgs.gov | 2014 |
| Annual wet day frequency | IMD | 1960-2019 |
| Dam location | Water resource information system, India | 2019 |
| River network | Open street map (OSM) from Survey of Inda (https://www.surveyofindia.gov.in/) | 2020 |
| Wetland location | Open street map (OSM) from Survey of Inda (https://www.surveyofindia.gov.in/) | 2020 |
| Education index | Odisha economic journal (http://www.orissaeconomicjournal.in/) | 2019 |
| Health index | | |
| Income index | | |
| Net irrigated area | Ground water booklet, Odisha | 2016 |
| Net water availability | Ground water booklet, Odisha | 2017 |

frequency of extreme drought (%) of 3, 6, 12 and 24 months, magnitude of drought of 3, 6, 12 and 24 months, mean intensity of drought of 3, 6, 12 and 24 months, return period of extreme drought of 3, 6, 12 and 24 months, return period of severe drought of 3, 6, 12 and 24 months, critical rainfall, yearly average rainfall, rainfall trend and vegetation condition index (VCI) are some of the indicators used to measure exposure (Fig. 3). The Standard Precipitation Index was used to calculate severity and frequency of extreme drought, magnitude of drought, mean intensity of drought and extreme and severe drought return periods. Where the rainfall was high, the drought effect was low. When the requirement for rainfall was higher, the chances of drought were high in that particular area. By the frequency, magnitude, intensity and return period of severe and extreme drought, the occurrence of a drought scenario in a specific area can be determined.

**2.3.1.1 Standard Precipitation Index (SPI)** To gauge the severity of the drought, the SPI value was calculated (McKee et al. 1993). The WMO authorised this index. Only the rainfall is required to calculate SPI. This rainfall data were used to calculate the drought for a variety of time periods, including 48, 24, 12, 6, 3 and SPI-1 months (Mehr and Vaheddoost 2020). Specific SPIs were estimated by using the precipitation data and the equation given by McKee et al. (1993) in the environment of R.

Only the classifications of severe and extreme drought were utilised to determine the severity of drought incidence in Odisha (Table 3). The droughts have been categorized

**Table 2** Factors selected for drought vulnerability modelling with causes and references

| Vulnerability indicators | Factors | Reason for selection | References |
|---|---|---|---|
| Exposure | Extreme drought frequency of 3, 6, 12 & 24 months | The increases of drought frequency reduce the crop productivity and impact on socio-economic status | Lin et al (2020); Zhang et al (2013) |
| | Severe drought frequency of 3, 6, 12 & 24 months | The increases of drought frequency reduce the crop productivity and impact on socio-economic status | Cao et al (2021); Mirgol et al (2021) |
| | Drought Magnitude of 3, 6, 12 & 24 months | High magnitude of drought largely influences the crop productivity as well as economic status of the farmers | Sharma & Panu, (2021); Abbas and Kousar (2021) |
| | Mean drought intensity of 3, 6, 12 & 24 months | High intensity of drought largely influences the crop productivity as well as economic status of the farmers | Jiang et al (2021); Masanta & Srinivas (2022) |
| | Return period of extreme drought of 3, 6, 12 & 24 months | The level of vulnerability to drought will be less if the return period is longer | da Rocha Júnior et al (2020); Nabaei et al (2019) |
| | Return period of severe drought of 3, 6, 12 & 24 months | The level of vulnerability to drought will be less if the return period is longer | Amrit et al (2018) |
| | Average rainfall | Less amount of rainfall increase the proneness of drought vulnerability | Ogunrinde et al (2019); Rahman & Dawood (2018) |
| | Critical rainfall | More the rainfall required will increase drought chances | Payab & Türker (2018) |
| | Rainfall trend | Negative trend indicates the dry condition intensification | Ouatiki et al (2019); Swain et al (2021a, b) |
| | VCI | Values of VCI indicate the dryness of an area | Sun et al. (2019); Feng et al (2019a, b) |
| Sensitivity | Evaporation | Regions having high evaporation rate are more prone to drought hazard | Dai et al (2018) |
| | Aridity index | Areas having higher intensity of aridity are more susceptible to drought | Tsiros et al (2020) |
| | Altitude | Higher altitude region are more susceptible for drought because of high surface runoff, higher slope induced soil erosion | Mbiriri et al (2018) |
| | Annual wet day frequency | More the frequency causes more risk of drought occurrences | Zhang et al (2021) |
| | Soil texture | Coarse soil texture region are more prone to drought because of high infiltration rate and low water retention capacity | Patel et al (2021) |
| | Slope | Sloppy areas are more prone to agricultural drought due to high surface runoff and high soil erosion | Zhang et al (2022) |
| | Bare soil index | More bareness means more prone to drought condition | Fadhil (2011) |
| | Trend of temperature | Positive trend is related with dry weather which intensifies the drought condition | Liang et al (2014) |
| | Total water use | More total water use, more vulnerability | Ullah et al (2019) |
| | Total water demand | More the water demand more the vulnerable to drought | Zhang et al (2019) |
| | Small and marginal farmers | More Small and marginal farmers are more vulnerable to drought | Brahmachari et al (2019) |
| | Population density | More population density, more vulnerability ot drought | Nasrollahi et al (2018) |
| | Net sown area | More the net sown area more the vulnerability to drought | Balaganesh et al (2020) |
| | Irrigation intensity | Lower irrigation intensity increases drought probability | Yu et al (2018) |
| | Cropping intensity | High cropping intensity area require huge amount of water for irrigation | Dar et al (2020) |
| Adaptive capacity | Distance from river | Nearer to the river drought vulnerability is less because of having good water accessibility | Swain et al (2022) |
| | Distance from dam | Nearby areas of the dam has less drought vulnerability because of more accessibility to water | Chai et al (2019) |
| | Distance from wetland | Neighbouring areas of the wetlands decreases can use the water from the wetlands and reduce the vulnerability to drought | Stirling et al (2020) |

**Table 2** (continued)

| Vulnerability indicators | Factors | Reason for selection | References |
|---|---|---|---|
| | Educational index | More education index, less vulnerability | Nübler et al (2021 |
| | Health index | High health index value indicates the good availability of medical facilities. Higher health facility will reduce drought impact | Machado-Silva et al (2020); Mehdipour et al (2022) |
| | Income index | Lower income grouped people are more affected by the drought | Belesova et al (2019) |
| | Net irrigated area | More irrigated area, less vulnerability | Meza et al (2020) |
| | Net water availability | Stored water can be used for irrigation to reduce the effect of drought | Zhang et al (2018) |
| | NDWI | Higher wetness area are less susceptible for drought | Shashikant et al 2021); Marusig et al 2020) |
| | NDVI | More vegetation cover reduces drought vulnerability | Nanzad et al (2019); Liu et al (2018) |

**Table 3** Drought classification using SPI values

| Values | Drought classes |
|---|---|
| More than 0 | Non-Drought |
| 0 to − 1.0 | Mild Drought |
| − 1.0 to − 1.5 | Moderate Drought |
| − 1.5 to − 2.0 | Severe Drought |
| Less than -2 | Extreme Drought |

based on drought classification values of SPI given by McKee et al. (1993). The periods of the SPI utilised in the study were 3, 6, 12 and 24 months since it effectively depicts long-term rainfall conditions and may be used to calculate reservoir levels, stream flows and levels of groundwater. The frequency of intense and severe droughts is computed as a percentage using the formula:

$$DF_{i,100} = \frac{N_i}{i.n} \times 100 \quad (1)$$

where $DF_{i,100}$ represents the drought frequency number for time scale I (3, 6, 12 and 24 month) in 100 years; $N_i$ denotes the figure of drought months for a i time scale within the of n year set; i = time scale (i.e., 6, 12 and 24 months). Cumulative water stress was represented by drought magnitude throughout the period of drought, and the average of this cumulative scarcity of water throughout the period of drought was denoted by mean drought intensity (MID) (Dayal et al. 2018). Thus, MD and MID can be computed using Eqs. 2and3, as follows:

$$MD = \sum_{j=1}^{x} SPI_{ij} \quad (2)$$

$$MID = \frac{MD}{m} \quad (3)$$

SPIij denotes the SPI values for a specific time scale j (3, 6, 12 and 24 month) and m denotes the month number. The California approach was applied using the Eq. 4 (Wable et al. 2019) to calculate the recurrence interval (RI) of severe and extreme drought. All values of SPI were sorted in rising order, and a rank was assigned to all SPI values.

$$RI = \frac{n}{p} \quad (4)$$

where n is the number of occurrences, and p is the event's rank.

Linear regression was used to assess the rainfall trend (Panda and Sahu 2019). Critical or threshold of rainfall is defined as the total amount of rain below which the drought will occur (Ghosh, 2019). The Eq. 5 was used to compute critical rainfall or threshold rainfall, as follows:

$$CR = \sigma SPI + \overline{X} \quad (5)$$

where, **σ** indicates the Standard Deviation of rainfall. The value of SPI is equivalent to -1.5. Average value of rainfall is indicated by the $\overline{X}$. The SPI value "−1.5" is considered as the threshold rainfall value.

Equation 6 has been utilised for calculating the vegetation condition index (VCI). The state of vegetation is generally expressed as a percentage. VCI levels around 0 (zero) percent indicate severe dryness, and VCI values from 50 to 100% represent typical vegetative conditions. Drought circumstances were indicated by a VCI of less - than 50%, whereas severe drought situations were indicated by a VCI of 0% to 35%.

$$VCI = \frac{NDVI_i - NDVI_{min}}{NDVI_{max} - NDVI_{min}} \times 100 \quad (6)$$

where, NDVIi represents the value of NDVI for a single pixel in the $_i$ month. $NDV_{Imax}$ and $NDVI_{min}$ are the

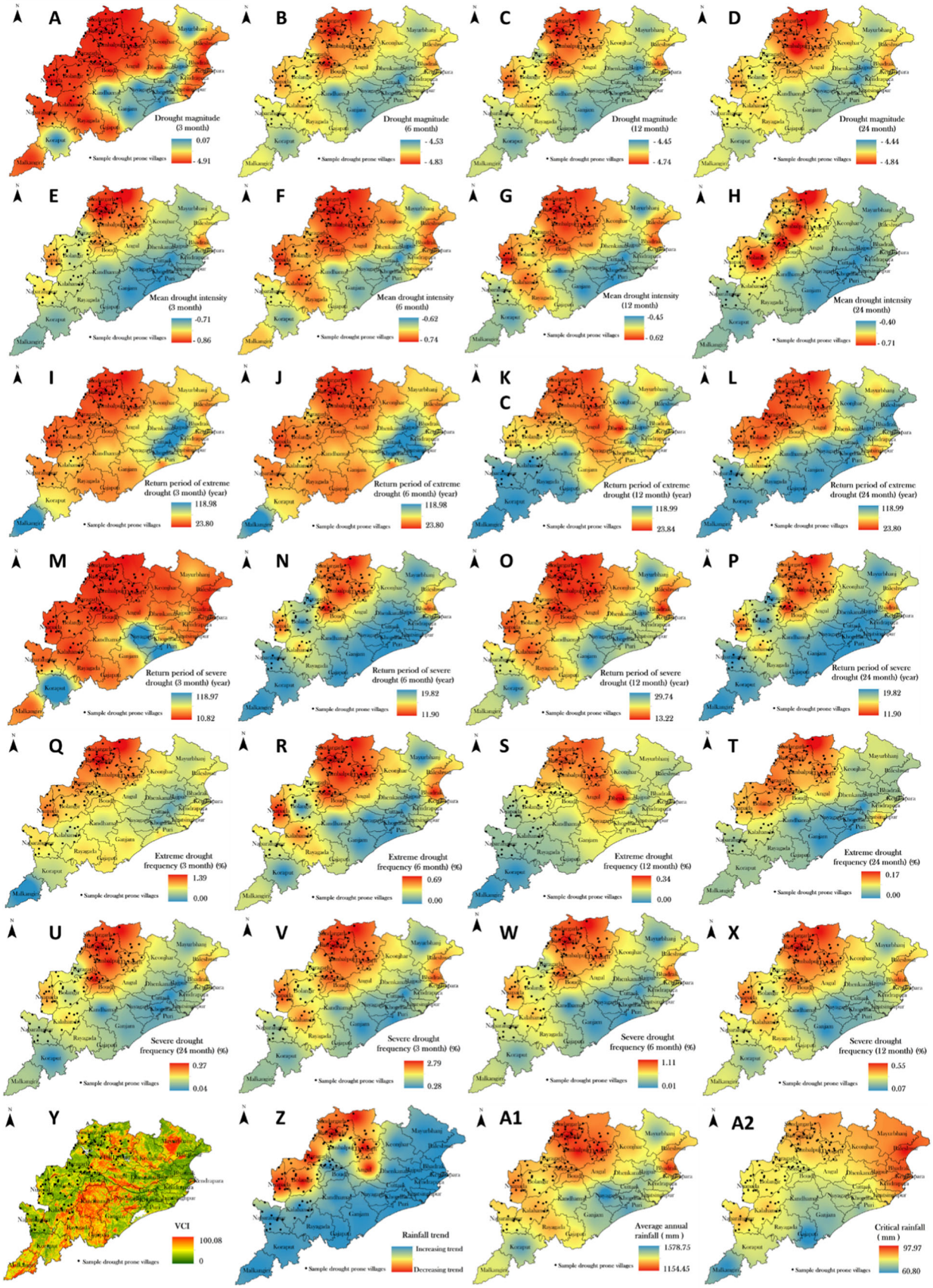
A
Drought magnitude (3 month)
0.07
- 4.91
B
Drought magnitude (6 month)
- 4.53
- 4.83
C
Drought magnitude (12 month)
- 4.45
- 4.74
D
Drought magnitude (24 month)
- 4.44
- 4.84
E
Mean drought intensity (3 month)
-0.71
- 0.86
F
Mean drought intensity (6 month)
-0.62
- 0.74
G
Mean drought intensity (12 month)
-0.45
- 0.62
H
Mean drought intensity (24 month)
-0.40
- 0.71
I
Return period of extreme drought (3 month) (year)
118.98
23.80
J
Return period of extreme drought (6 month) (year)
118.98
23.80
K
C
Return period of extreme drought (12 month) (year)
118.99
23.84
L
Return period of extreme drought (24 month) (year)
118.99
23.80
M
Return period of severe drought (3 month) (year)
118.97
10.82
N
Return period of severe drought (6 month) (year)
19.82
11.90
O
Return period of severe drought (12 month) (year)
29.74
13.22
P
Return period of severe drought (24 month) (year)
19.82
11.90
Q
Extreme drought frequency (3 month) (%)
1.39
0.00
R
Extreme drought frequency (6 month) (%)
0.69
0.00
S
Extreme drought frequency (12 month) (%)
0.34
0.00
T
Extreme drought frequency (24 month) (%)
0.17
0.00
U
Severe drought frequency (24 month) (%)
0.27
0.04
V
Severe drought frequency (3 month) (%)
2.79
0.28
W
Severe drought frequency (6 month) (%)
1.11
0.01
X
Severe drought frequency (12 month) (%)
0.55
0.07
Y
VCI
100.08
0
Z
Rainfall trend
Increasing trend
Decreasing trend
A1
Average annual rainfall ( mm )
1578.75
1154.45
A2
Critical rainfall ( mm )
97.97
60.80
Sample drought prone villages

◀**Fig. 3** Factors of exposure: Drought magnitude- **A** 3 month, **B** 6 month, **C** 12 month, **D** 24 month, Mean drought intensity- **E** 3 month, **F** 6 month, **G** 12 month, **H** 24 month, Return period of extreme drought- **I** 3 month, **J** 6 month, **K** 12 month, **L** 24 month, Return period of severe drought- **M** 3 month, **N** 6 month, **O** 12 month, **P** 24 month, Extreme drought frequency -**Q** 3 month, R. 6 month, S. 12 month, **T** 24 month, Severe drought frequency - **U** 3 month, **V** 6 month, **W** 12 month, **X** 24 month, **Y** Vegetation condition index (VCI), **Z** Rainfall trend, $A_1$. Average annual rainfall and $A_2$. Critical rainfall

maximum and minimum NDVI values for the same pixel, respectively. The VCI has been used to analyse the geographical features of drought, but prior research has seldom assessed its efficacy in detecting and distinguishing water-stressed farmland from other plants. (Table 3)

### 2.3.2 Sensitivity indicators

Cropping intensity, irrigation intensity, net sown area, population density, small and marginal farmers, total water demand, total water use, temperature trend, bare soil index (BSI), slope, evaporation, aridity index, soil texture, altitude and annual wet day frequency were the sensitivity factors (Fig. 4). These factors affected how exposure would manifest; for example, when a region's population grew, more individuals would be exposed to drought, increasing the region's vulnerability (Naumann et al. 2019). Evaporation and temperature are two of the most important meteorological variables that influence land cover, ecological sustainability and water balance (Ekwueme and Agunwamba 2020). Both biophysical and economic variables are included in this class of sensitivity. Temperature is a key determinant of drought sensitivity (Mega et al. 2019). As the temperature rises, drought becomes more prevalent (Shi et al. 2021). In this study, the temperature trend was calculated using linear regression. Total water usage was linked to drought vulnerability, since water demands in areas with high water use are likely to be greater during dry years. Therefore, regions with considerably higher water usage would experience more dry seasons than regions with lower water use. Cropping intensity is defined as the ratio of net cropped area to gross cropped area. According to Potopová et al. (2021), crop intensity and drought intensity increase together. In areas where there is a lack of water, a drought might be disastrous (Bakht et al. 2020). Domestic water use, agricultural water use, animal water use, and industrial water requirements are all added together to get the overall water demand. Drought will affect marginal and small farmers more severely if their numbers are high (Venancio et al. 2020). Small farmers will be more affected by drought conditions than large farmers since most of them utilise low-tech production techniques and have limited agricultural area. The net planted area can also be used to estimate drought vulnerability. Drought will have a greater impact on agriculture with the growth of the net sown area and vice versa. As the aridity index value increases, the dryness will increase, but dryness will decrease as the aridity index value decreases (Wu et al. 2021).

$$Aridityindex(AI) = \frac{PET - AET}{PET} \times 100 \quad (7)$$

where, the PET stands for the potential evapotranspiration and AET stand for actual evapo-transpiration. Thus, the drought effect is higher in areas with high aridity (Yves et al. 2020). On one hand, when the soil is open or bare, the area will be highly affected by drought; on the other hand, the area covered by vegetation will be relatively protected from the effect of drought (Sankaran 2019). The bareness of the soil is calculated by using the BSI. It is a numerical indicator that normalises the blue, red, near-infrared, and short-wave-infrared spectral bands of a multispectral picture. The spatial picture of soil bareness is obtained by combining those bands in a defined fashion (Eq. 8), and it is utilised as the sensitivity data layer (Fig. 2g) for this investigation, as follows:

$$Baresoilindex(BSI) = \frac{(b_{SWIR} + b_R) - (b_{NIR} + b_B)}{(b_{SWIR} + b_R) + (b_{NIR} + b_B)} \quad (8)$$

where, $b_{SWIR}$ stands for short-wave infrared band brightness, $b_R$ for red band brightness, $b_{NIR}$ for near-infrared band brightness and $b_B$ for blue band brightness. A coarser soil texture cannot hold the moisture in the top layer. Consequently rain water will penetrate deep into the soil. The top layer of the soil will remain dry. So, this area will be more affected by drought events. On the contrary, if the soil texture is fine, then the soil will hold the water in the top layer, and the top layer will remain wet. So, this area will be less affected by the drought event. Annual wet day frequency is the most significant indicator of drought. The likelihood of a drought decreasing as the number of wet days in a year increases and vice-versa.

### 2.3.3 Adaptive capacity

The inadequacy of a population group to react adequately to a certain widespread stressor is how vulnerability is typically defined (Cianconi et al. 2020). As a result, social vulnerability refers to a population group's vulnerability as a result of the deficit of resources with which to react to a hazard (Antronico et al. 2020). Consequently, environmental indicators of adaptation capability, such as distance from river, distance from wetland, net water availability, NDWI and NDVI, and socio-economic factors, such as distance from dam, net irrigated area, income index, health index and education index, were included in this study. These factors demonstrate the population's capacity to

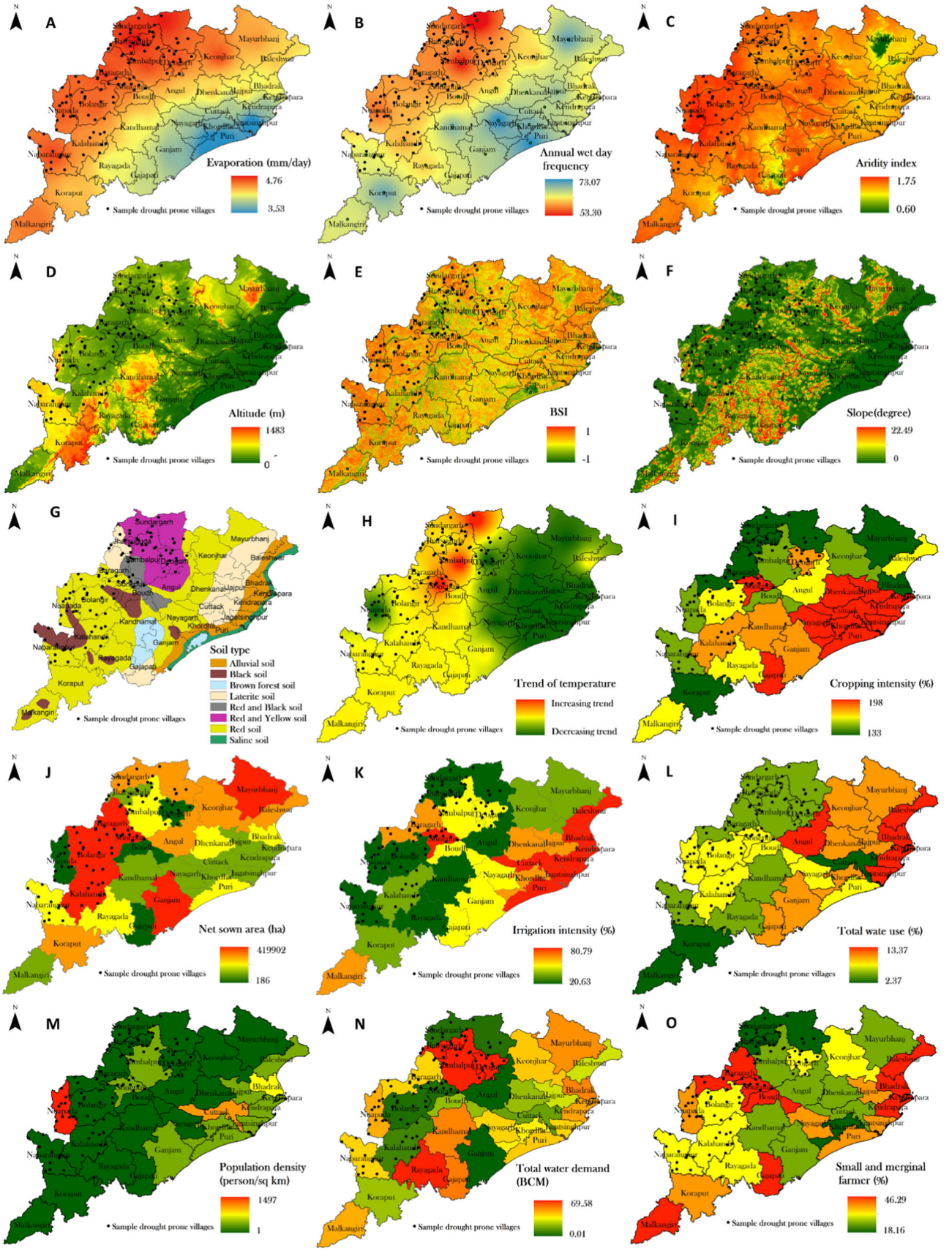
A
Evaporation (mm/day)
4.76
3.53
B
Annual wet day frequency
73.07
53.30
C
Aridity index
1.75
0.60
D
Altitude (m)
1483
0
E
BSI
1
-1
F
Slope(degree)
22.49
0
G
Soil type
Alluvial soil
Black soil
Brown forest soil
Laterite soil
Red and Black soil
Red and Yellow soil
Red soil
Saline soil
H
Trend of temperature
Increasing trend
Decreasing trend
I
Cropping intensity (%)
198
133
J
Net sown area (ha)
419902
186
K
Irrigation intensity (%)
80.79
20.63
L
Total wate use (%)
13.37
2.37
M
Population density (person/sq km)
1497
1
N
Total water demand (BCM)
69.58
0.01
O
Small and merginal farmer (%)
46.29
18.16
• Sample drought prone villages

◀**Fig. 4** Factors of sensitivity maps: **A** Evaporation, **B** Annual wet day frequency, **C** Aridity index, **D** Altitude, **E** BSI, **F** Slope, **G** Soil texture, H. Trend of temperature, **I** Cropping intensity, **J** Net sown area, **K** Irrigation intensity, **L** Total water use, **M** Population density, **N** Total water use, **O** Small and marginal farmer

respond to a drought situation (Fig. 5). Higher availability of irrigation facility reduces drought vulnerability, because it fulfils the water demand during dry season. Drought cannot readily affect regions when vast volumes of water are available at all times of the year (Mafi-Gholami et al. 2020). If there is insufficient rain in a particular location with high water availability, then the region may make up the shortfall by using available water sources. Such areas will experience drought if there are no other water supplies available than rainfall. The health, wealth, and level of education of the local people strongly influence drought susceptibility. If a region's health, education, and economic possibilities improve, drought vulnerability will diminish (Phelps and Kelly 2019). The more away from dams, rivers, and wetlands a place is, the more susceptible it is to drought conditions; this is because the supply of water declines with increasing distance from the dam, the river and the wetlands (Moser et al. 2019). The area is protected from dryness by a dense plant cover (Helcoski et al. 2020). Bare terrain is more susceptible to drought. If the NDVI value is closer to 1, then a significant quantity of plant cover is available. If the value is closer to -1, then a very small amount of vegetation cover is available. The NDVI is calculated (Eq. 9) using Landsat 8 Operational Land Imager (OLI) imagery, as follows:

$$NDVI = \frac{NIR - R}{NIR + R} \tag{9}$$

NDWI is an important parameter for identifying drought situations, because the moisture or water condition can be represented by this index (Marusig et al. 2020). Mcfeeters in 1996 developed the NDWI approach to represent water bodies based on the fact that water has the highest absorption, and vegetation has the highest reflectance in near infrared (Ety et al. 2021).

$$NDWI = \frac{Green - NIR}{Green + NIR} \tag{10}$$

## 2.4 Machine learning models for drought vulnerability mapping

### 2.4.1 M5P

Quinlan in 1992 proposed M5P, a regression technique that is tree-based. It provides values for future prediction according to trees' leaves (Ünlü 2020). This technique generates trees that use multivariate linear algorithms. This method can solve problems with a large dimensionality of 100 characters. By constructing smaller trees, it is more effective and produces results with more accuracy. Rather than discrete variables, this approach uses continuous variables (Talukdar et al. 2020). A detailed analysis of this method can be found in Talukdar et al. (2020).

### 2.4.2 Dagging

Another ensemble machine learning (EML) approach used to generate meta-learners is the dagging algorithm, and it is often called disjoint aggregating (Zounemat-Kermani et al. 2021). Dagging is comparable to bagging, but the sampling technique is different. Rather than using bootstrap sampling, this technique uses the disjoint sampling approach to obtain randomised training sections from the actual dataset without replacing them (Barzegar et al. 2021). Finally, the different output models derived from disjunct samples are combined using the methodology of the majority vote.

### 2.4.3 Random Subspace (RSS)

RSS was introduced in 1988 to enhance the reliability of weaker classifications and the performance of individual classifications. RSS is a common approach for random selection, in which the main character varies at random (Costello and Lee 2020). RSS has been utilised in a variety of disciplines, including economics and medical, but very seldom in potential groundwater determination.

### 2.4.4 Rotation Forest (RTF)

An EML classifier, RTF is a generating approach that aims to provide a wide range of precise classifiers within the ensemble (Subasi et al. 2019). This process utilises the bootstrapping sampling method and trains the decision trees; it is separately dependent on constructing a classifier ensemble to use a future extracting approach, such as the principal component analysis (PCA), which is comparable with the ideas of bagging approaches. In Rotation Forest, retrieving features were utilised for every one of the basic classifiers to sustain variety (Geran Malek et al. 2021). Each one of the base classifiers is trained on the whole dataset in the rotated feature space to optimise individual efficiency. The model parameters are randomly divided into subgroups, and every subset is subjected to feature excavation (Table 4). The ultimate result is obtained by merging most of the trees' mean outputs.

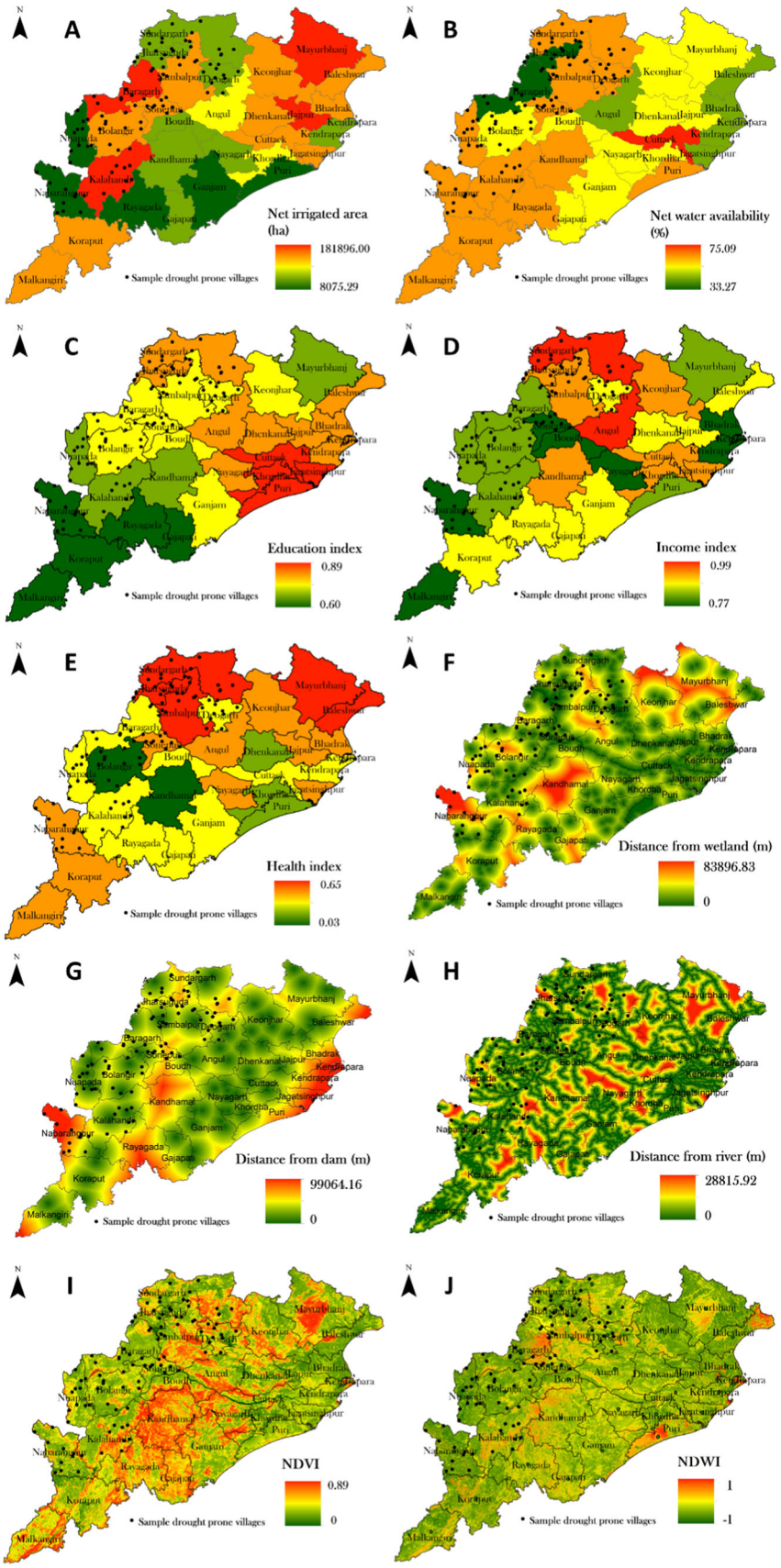


**Fig. 5** Factors of adaptive capability maps: **A** Net irrigated area, **B** Net water availability, **C** Education index, **D** Income index, **E** Health index, **F** Distance from wet land, **G** Distance from dam, **H** Distance from river **I** NDVI, **J** NDWI

**Table 4** Description of models' parameters

| Model | Parameters' description |
|---|---|
| Dagging | Base classifer-M5P, max depth- -1, minimum number-2, minimum proportion of variance-0.001, seed-3, number of fold-10 and Number of iterations, 16 |
| Random Subspace | Base classifer-M5P, max depth- -1, minimum number-2, minimum proportion of variance-0.001, seed-, number of execution slots-1 and Number of iterations-20, size of subspace-0.5 |
| RTF | Number of iterations, 4; seed, 2; minimum size of group, 3; maximum size of group, 3; minimum proportion of variance-0.001, projection filter, a principal components analysis; use a base classifier-M5P |

#### 2.4.5 Ensemble of models

Nguyen et al. (2020) defined ensemble modelling as a strategy for combining the impacts of many models into a single embedded model to improve prediction capacity. This technique has attracted the attention of academics working on specific machine learning and data mining models. Seni and Elder (2010) described the creation of ensemble models by using the weighted integration of a single model. However, the method used for calculating these weights is complicated. In this study, for ensembling the models, M5P was used as base classifier, and RTF, RSS and Dagging were used as meta classifiers. Ensemble meta classifiers have been used to optimise the input data using training dataset before creating drought vulnerability models. The basis classifier of M5P has then been applied to identify classes for drought vulnerability spatial prediction using optimized input data. Finally, models for drought vulnerability have been developed using machine learning ensemble frameworks. Maps of drought vulnerability have been created using the results of training drought models.

### 2.5 Validation of drought vulnerability models

#### 2.5.1 Receiver operating characteristics (ROC)

Validation is a crucial step in determining the scientific relevance of a completed study (Hribar et al. 2018; Hong et al. 2018). The area under curve (AUC)-ROC was used by experts to examine the predictive ability of the models. Graphical representation of a model achievement as indicated by a diagnostic assessment is displayed by the ROC (Heldt et al. 2021). The correct (drought-impacted zone) and the erroneous (non-drought-impacted zone) predictions are represented on the Y and X axes, respectively. The AUC was used to assess the models' predictions. The AUC ranges from 0 to 1 with a value nearer to 1, thereby indicating a model's ability to predict effectively (McCune, et al. 2020).

#### 2.5.2 Precision

When similar data are assessed frequently, the extents of the estimated values are similar to one another. Precision represents the degree of random deviations in the estimation process (Reynolds et al. 2021).

$$\Pr ecision = \frac{TP}{FP + TP} \tag{11}$$

where, $TP$ = True positive value, $FP$ = False positive value.

#### 2.5.3 Root mean square error

The employed models' predictive power was assessed using the ROC and precision, while the predictive model error was assessed using the RMSE and MAE (Salih et al. 2020).The RMSE was determined by comparing observed data in the field with projected values provided by the model (Willmott et al., 2005). The following formula was used to determine the RMSE value:

$$RMSE = \sqrt{\frac{\sum_{i=1}^{N} (O_i - S_i)^2}{n}} \tag{12}$$

$Oi$ and $Si$ are the values of anticipated and observed, respectively. The entire amount of data points is denoted by n.

#### 2.5.4 MAEI

MAE is similar to RMSE in that it is calculated as the sum of differences between model-predicted values and field observed values, but it does not consider the direction of the differences (Willmott et al., 2005) (Eq. 13), as follows:

$$MAE = \frac{\sum_{i=1}^{n} |S_i - O_i|}{n} \tag{13}$$

Oi and Si are the values of anticipated and observed, respectively. The entire amount of data points is denoted by the letter n.

#### 2.5.5 K-index

This coefficient is being used to determine how accurate a categorisation is. Kappa is a measure of how well a categorisation performs compared with randomly assigning values (Silva and Eugenio Naranjo 2020). The kappa coefficient might be anything between− 1 and 1. A value of 0 indicates that the categorisation is not superior to the arbitrary (Ghada et al. 2019). A negative number indicates that the categorisation is less accurate. A positive value means that the classification is superior to random classification.

#### 2.5.6 Friedman and Wilcoxon rank test

In 1937, Friedman created a non-parametric test to identify substantial differences between two applied models (Miraki et al. 2019). If the *P*-values are $< 0.05$, then the alternative hypothesis is accepted, thereby implying that a substantial difference exists among the predictions of models (Chung et al. 2019). Researchers employed the Wilcoxon rank test, which enables them to evaluate the methodical degree of significant variations inside the RDV models (Tien Bui et al. 2016). The models were easily distinguished since the alternative hypothesis was not ruled out if the z-value was greater than + 1.96 or − 1.96 with a *p* value of 0.05. (Tien Bui et al. 2018).

## 3 Result

### 3.1 Exposure mapping using ensemble models

The four MLAs were used to create the exposure maps (Fig. 6). By using the natural-break method, each model's anticipated drought exposure was divided into five exposure classes (Hoque et al. 2021). The north western and western parts of the research region were highly exposed to drought. The high and very-high exposure zones for the M5P model encompassed 10.80% and 24.71% of the state. Except for the north-western and western parts of the state, very-low, low and moderate exposure zones accounted for 19.52%, 34.15% and 10.80% of the total area, respectively (Table 5). For the model of M5P-Dagging, very-low and low exposure areas captured 47.79% of the total area in the eastern to southern part. The high and very-high exposure zones comprised 33.09% of the total land on the western and north western sides. The north eastern and central parts

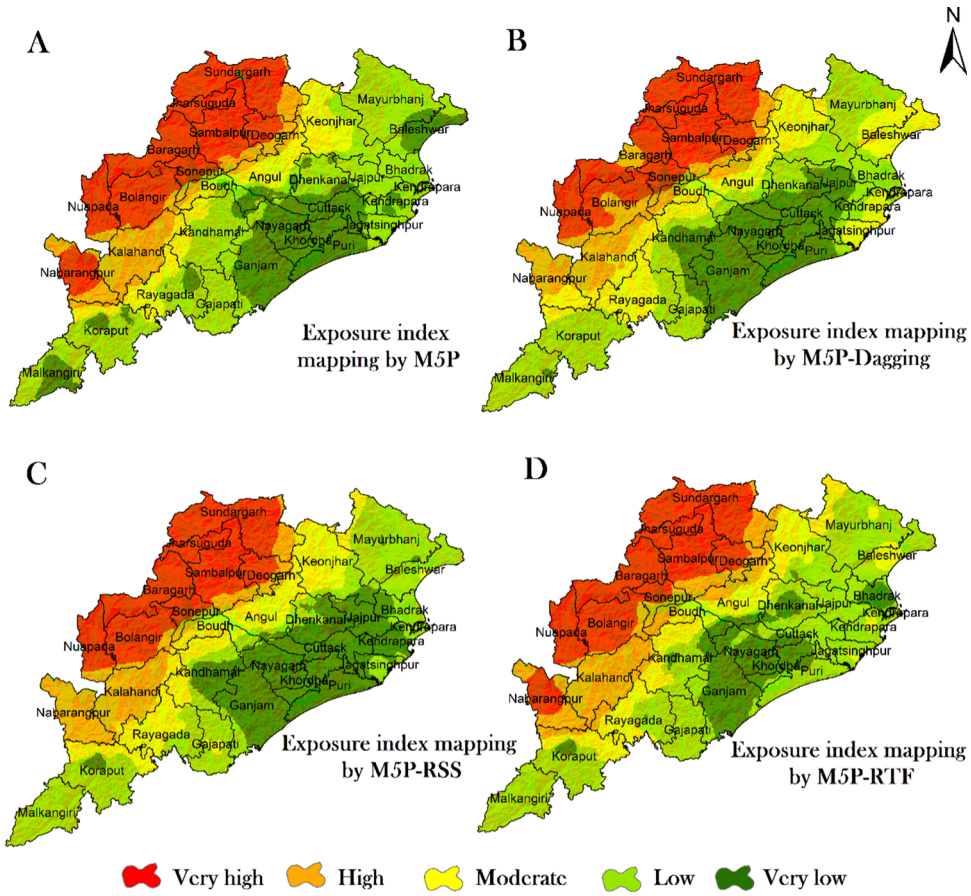


**Fig. 6** Exposure index maps produced by: **A** M5P, **B** M5P-Dagging, **C** M5P-RSS, and **D** M5P-RTF

**Table 5** Area under different exposure classes for every considered model

| Models | Exposure class | Area (%) | Area in (sq. km) |
|---|---|---|---|
| M5P | Very low | 19.52 | 30,408.84 |
| | Low | 34.15 | 53,181.94 |
| | Moderate | 10.80 | 16,817.90 |
| | High | 10.80 | 16,822.09 |
| | Very high | 24.71 | 38,476.23 |
| M5P—Dagging | Very low | 19.52 | 30,408.84 |
| | Low | 27.10 | 42,206.09 |
| | Moderate | 20.26 | 31,557.13 |
| | High | 11.64 | 18,133.83 |
| | Very high | 21.45 | 33,401.11 |
| M5P- RSS | Very low | 22.72 | 35,379.19 |
| | Low | 26.26 | 40,898.55 |
| | Moderate | 16.91 | 26,339.52 |
| | High | 12.05 | 18,770.84 |
| | Very high | 22.04 | 34,318.91 |
| M5P-RTF | Very low | 12.58 | 19,600.63 |
| | Low | 34.92 | 54,384.72 |
| | Moderate | 14.61 | 22,752.15 |
| | High | 14.43 | 22,475.55 |
| | Very high | 23.43 | 36,493.96 |

were occupied by a moderate exposure zone (20.26%) (Table 5). In the north western and western parts of the study region, the high and very-high exposure zones for the M5P-RSS model comprised 12.05% and 22.04% of the study area, respectively. Very-low, low and moderate exposure zones accounted for 22.72%, 26.26% and 16.91% of the total area, respectively. For the model of M5P-RTF, very-low and low exposure areas captured 73,985.35 sq. km of the total area. The high and very-high exposure zone comprised 58,969.51 sq. km. of the total land. An isolated pocket in the north eastern part and the total central part was occupied by a moderate exposure zone (22,752.15 sq. km.). All the models showed high areal coverage of very-high and high exposure zones in the north-wester and western parts of the state due to the frequent occurrence of meteorological and agricultural drought.

## 3.2 Sensitivity mapping using ensemble models

The same four MLAs were used to create the sensitivity maps (Fig. 7). With the aid of natural-break method, each model's anticipated drought sensitivity was divided into five sensitivity classes, the same as exposure. In the north-western and western parts of the study area, the high and very-high sensitivity zones for the M5P model encompassed 17.16% and 21.10% of the state, respectively. Very-low, low and moderate sensitivity zones are accounted for 23.20%, 23.85% and 14.67% of the total area, respectively (Table 6). For the model of M5P-Dagging, very-low and low sensitivity areas captured 52.49% of the total area in the eastern to southern part. The high and very-high sensitivity zones comprised 32.40% of the total land on the western and north-western sides. The north-eastern and central parts were occupied by a moderate sensitivity zone (15.08%) (Table 6). In the north-western and western parts of the study region, the high and very-high sensitivity zones for the M5P-RSS model comprised 15.57% and 23.42% of the study area, respectively. Very-low, low and moderate sensitivity zones are accounted for 23.38%, 18.04% and 19.56% of the total area, respectively (Table 6). For the model of M5P-RTF, very-low and low sensitivity areas captured 76,422.36 sq. km of the total area in the eastern to southern part. The high and very-high sensitivity zones comprised 54,697.55 sq. km. of the total land on the western and north-western sides. The total central part was occupied by a moderate sensitivity zone (24,587.08 sq. km.) (Fig. 4). Owing to the high evaporation rate, increasing trend of temperature and high aridity, the sensitivity to drought was very high in the western part of the state, as shown by the all models.

## 3.3 Adaptive capability mapping by using ensemble models

To produce the adaptive capability maps, M5P, M5P-Dagging, M5P-RSS, and M5P-RTF ensemble models were also employed (Fig. 8). By using the natural-break method, each model's anticipated drought adaptive capability was divided into five adaptive capability classes, such as in exposure and sensitivity maps. In the north-western and western parts of the region, the high and very-high adaptive capability classes for the M5P model covered 12.03% and 3.73% of the study area, respectively. Except in the north-western and western parts of the research territory, very-low, low and moderate adaptive capability zones captured 10.94%, 36.85% and 36.42% of the total area, respectively (Table 7). For the model of M5P-Dagging, very-low and low adaptive capability areas captured 58.77% of the total area from the eastern to southern part. The high and very-high adaptive capability zone comprised 23.6% of the total land. The north-eastern and central parts were occupied by a moderate adaptive capability zone (17.60%). For the M5P-RSS model, the high and very-high adaptation capacity zones made up 25.37% and 7.62% of the research area, respectively. Zones with very low, low, and moderate adaptation capabilities make up, respectively, 11.79%, 38.83%, and 16.37% of the total area (Table 7). For the model of M5P-RTF, very-low and low adaptive capability

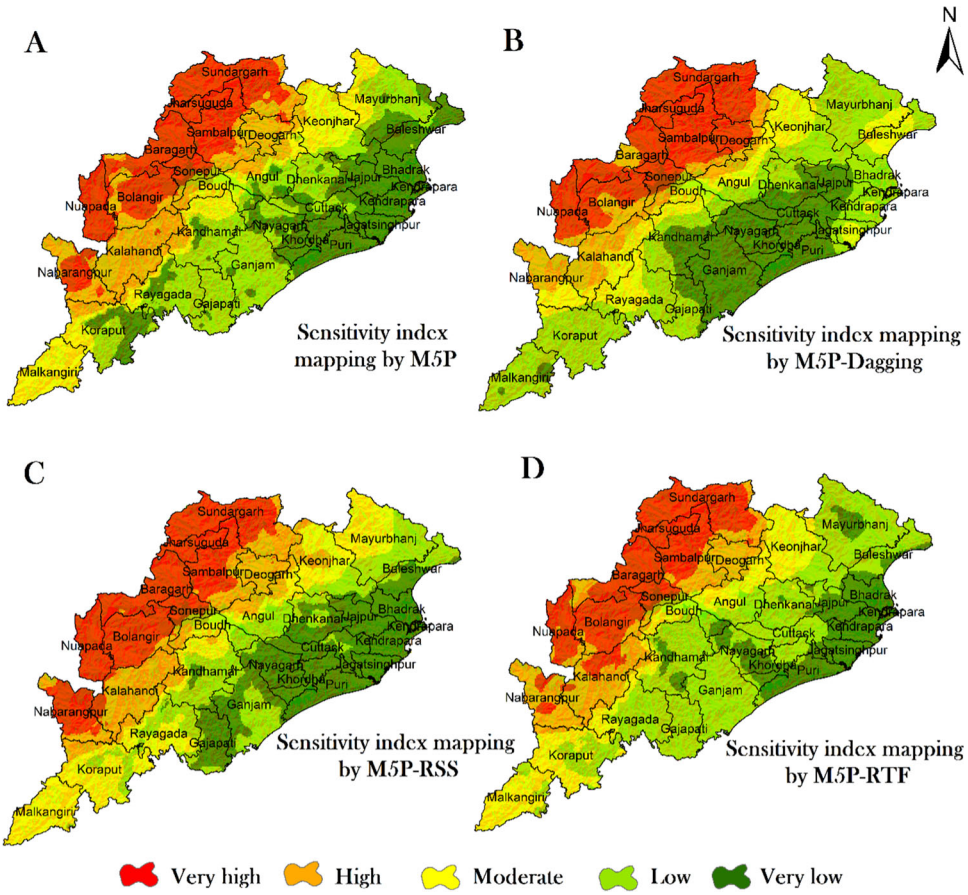


**Fig. 7** Sensitivity index maps produced by: **A** M5P, **B** M5P-Dagging, **C** M5P-RSS, and **D** M5P-RTF

areas captured 94,176.88 sq. km of the total area in the eastern to southern part. The high and very-high adaptive capability zones comprised 39,121.62 sq. km. of the total land on the western and north western sides. The entire central part was occupied by a moderate adaptive capability zone (22,408.50 sq. km.).

### 3.4 Vulnerability mapping by using ensemble models

The four ensemble models generated three indices, namely exposure, sensitivity, and adaptive capacity, which were then utilised to create maps of drought vulnerability (Fig. 9).The predicted drought vulnerability was categorised into five classes, namely, very-high, high, moderate, low and very-low by the natural break method. For the model of M5P, very-high to high vulnerability zones were found in the western and north western parts of the study region. These two zones occupied 35.6% of the study area. Very-low to low vulnerable areas were found along the north eastern to southern part of the map. These two zones occupied 51.96% of the area. A moderate vulnerable zone was found in the central part (12.41%) in between the very-high to high and very low to low vulnerable zones (Table 8). For the model of M5P-Dagging, very-low and low vulnerable areas captured 71,879.59 sq. km of the total area in the eastern to southern part. The high and very-high vulnerable zones comprised 62,400.14 sq. km. of the total land in the western and north-western part. The entire central part was occupied by a moderate vulnerability zone (21,427.26 sq. km.) (Table 8). In the north-western and western parts of the study region, the high and very-high vulnerable zones for the M5P-RSS model comprised 14.22%and 23.68% of the study area, respectively. Except in the north-western and western parts of the research region, very-low, low and moderate vulnerability zones accounted for 25.53%, 25.81% and 10.74% of the total area, respectively (Table 8). In the case of the model of M5P-RTF, very-low and low vulnerable areas covered 75,345.34 s q. km of the total area from the eastern to southern part. The high and very-high vulnerability zones occupied 59,030.78 sq. km. of the total land on the western and north western sides. The middle part of the map was under the zone of moderate vulnerability. (21,330.87 sq. km).

**Table 6** Area under different sensitivity classes for every considered model

| Models | Sensitivity class | Area (%) | Area in (sq. km) |
|---|---|---|---|
| M5P | Very low | 23.20 | 36,125.16 |
| | Low | 23.85 | 37,139.35 |
| | Moderate | 14.67 | 22,844.35 |
| | High | 17.16 | 26,733.46 |
| | Very high | 21.10 | 32,864.68 |
| M5P-Dagging | Very low | 21.00 | 32,709.62 |
| | Low | 31.49 | 49,045.57 |
| | Moderate | 15.08 | 23,481.36 |
| | High | 10.74 | 16,734.08 |
| | Very high | 21.66 | 33,736.38 |
| M5P- RSS | Very low | 23.38 | 36,418.52 |
| | Low | 18.04 | 28,099.68 |
| | Moderate | 19.56 | 30,471.70 |
| | High | 15.57 | 24,244.09 |
| | Very high | 23.42 | 36,473.00 |
| M5P-RTF | Very low | 13.57 | 21,133.91 |
| | Low | 35.50 | 55,288.45 |
| | Moderate | 15.79 | 24,587.08 |
| | High | 14.09 | 21,946.91 |
| | Very high | 21.03 | 32,750.64 |

### 3.5 Correlation between drought vulnerability and exposure, sensitivity and adaptive capacity indices

The vulnerability of an area is significantly associated with the exposure, sensitivity and adaptive capability of that area (Singha et al. 2020). To assess the relationship between drought vulnerability and the three indices of exposure, sensitivity and adaptive capability, the Pearson correlation method was used. Exposure and sensitivity indices were very strongly related with the overall drought vulnerability. The exposure index correlation values (r) ranged from 0.545 to 0.990. Sensitivity index r values ranged from 0.556 to 0.984 (Table 9). Adaptive capability index's association with overall drought vulnerability was not as high as those of exposure or sensitivity indices. Table 9 shows that the r values for all pairs were lower in the case of M5P-Dagging than in other applied models.

### 3.6 Comparison and validation between different models of drought vulnerability

Rationality evaluation is a crucial step in reaching a conclusion on the predictive ability of deployed models (Karstoft et al. 2021). The ROC, RMSE, MAE, precision, K-index, Friedman test and Wilcoxon test were used to compare and validate the models. The ROC curve results showed that in the case of training data, the AUCs for the RTF-M5P, RSS-M5P, M5P and DAG-M5P models were 0.873, 0.855, 0.842 and 0.805, respectively (Table 10). The result of the ROC curve showed that in the case of testing data set, the AUCs for the RTF-M5P, RSS-M5P, M5P and DAG-M5P models were 0.901, 0.874, 0.859 and 0.852, respectively (Fig. 10). As the ROC values ranged from 0.805 to 0.901, the four ensemble models had good prediction capabilities for generating the drought vulnerability map. However, the RTF-M5P model was the best fit for producing a map of drought vulnerability, because it had the highest AUC value in both training and testing (Table 10). RTF-M5P model had the lowest MAE (Training-0.269 and Testing-0.206) and RMSE (Training-0.146 and Testing-0.102) values. Moreover, the K-index value was found to be the highest (Training-0.879 and Testing-0.886) for the RTF-M5P. This model had a high precision rate (Training-0.873 and Testing- 0.889) (Table 11). All of the models had approximately comparable RMSE, MAE, precision and K-index values. Thus, all the models had almost identical drought vulnerability prediction capabilities, but the RTF-M5P model was the most suitable. According to the Friedman test (Table 12) the estimated Chi-square value was 11.936, and the p-value was 0.007, indicating the significant differentiation among the models. Similarly, Wilcoxon test shows the significant difference among the drought vulnerability indexed (Table 13).

## 4 Discussion

Drought is one of the most disastrous climatic hazards. It has a bad influence on the livelihood conditions in areas where most of the people are depended on agricultural activities. Many parts of India are frequently affected by drought almost every year. Odisha is one of the states frequently affected by this climatic hazard. Numerous scientists have conducted drought prevention and policy development research for India (Javadinejad et al. 2020; Sam et al. 2020). Studies were conducted in Odisha to identify the areas prone to drought; results indicated that drought is a serious concern (Senapati 2019; Saha et al 2021a). In most of the previous studies, researchers focused more on drought forecasting rather than drought vulnerability. However, for formulating the scientific strategies to reduce the effect of drought, an assessment of drought vulnerability that considers the various indicators of exposure, sensitivity and adaptive capacity is essential.

In this present study, drought vulnerability was evaluated using three different groups of parameters, namely,

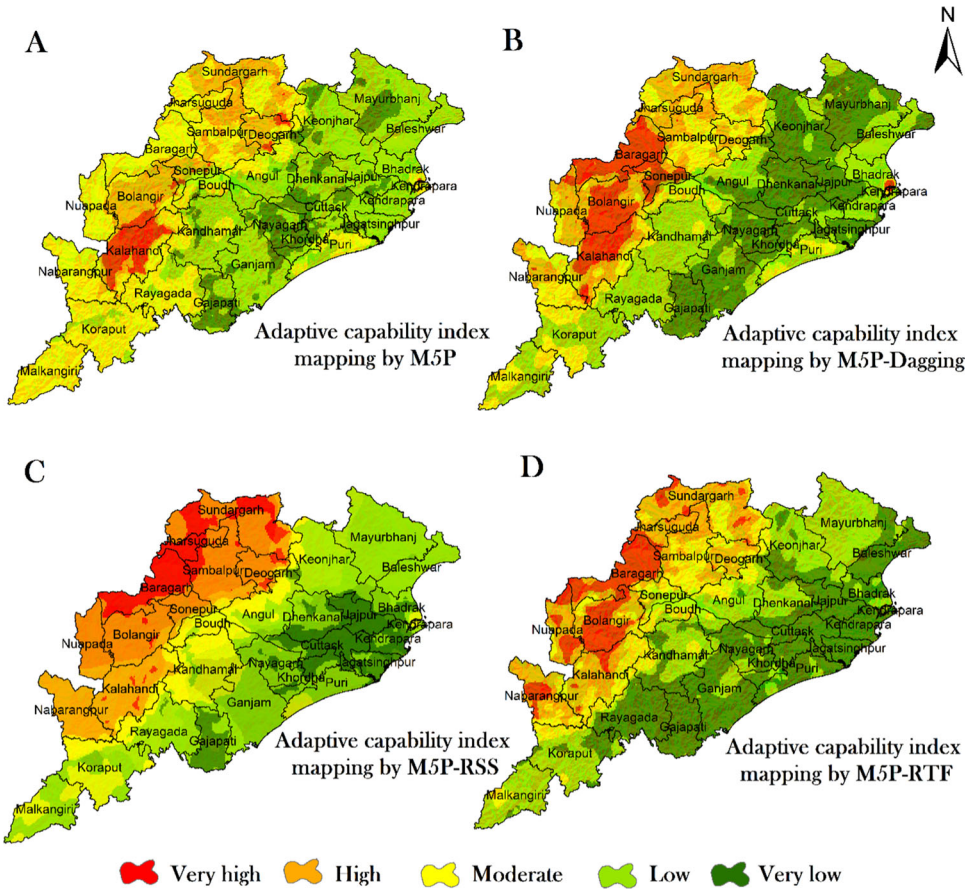


**Fig. 8** Adaptive capability index maps produced by: **A** M5P, **B** M5P-Dagging, **C** M5P-RSS, and **D** M5P-RTF

**Table 7** Area under different adaptive capability classes for every considered model

| Models | Adaptive capability class | Area (%) | Area in (sq. km) |
|---|---|---|---|
| M5P | Very low | 10.94 | 17,035.82 |
| | Low | 36.85 | 57,385.37 |
| | Moderate | 36.42 | 56,719.02 |
| | High | 12.03 | 18,745.69 |
| | Very high | 3.73 | 5821.10 |
| M5P—Dagging | Very low | 28.60 | 44,543.39 |
| | Low | 30.17 | 46,990.78 |
| | Moderate | 17.60 | 27,411.64 |
| | High | 14.10 | 21,967.87 |
| | Very high | 9.50 | 14,793.32 |
| M5P- RSS | Very low | 11.79 | 18,364.32 |
| | Low | 38.83 | 60,461.45 |
| | Moderate | 16.37 | 25,492.97 |
| | High | 25.37 | 39,515.57 |
| | Very high | 7.62 | 11,872.69 |
| M5P-RTF | Very low | 34.09 | 53,085.55 |
| | Low | 26.39 | 41,091.33 |
| | Moderate | 14.39 | 22,408.50 |
| | High | 16.39 | 25,526.49 |
| | Very high | 8.73 | 13,595.13 |

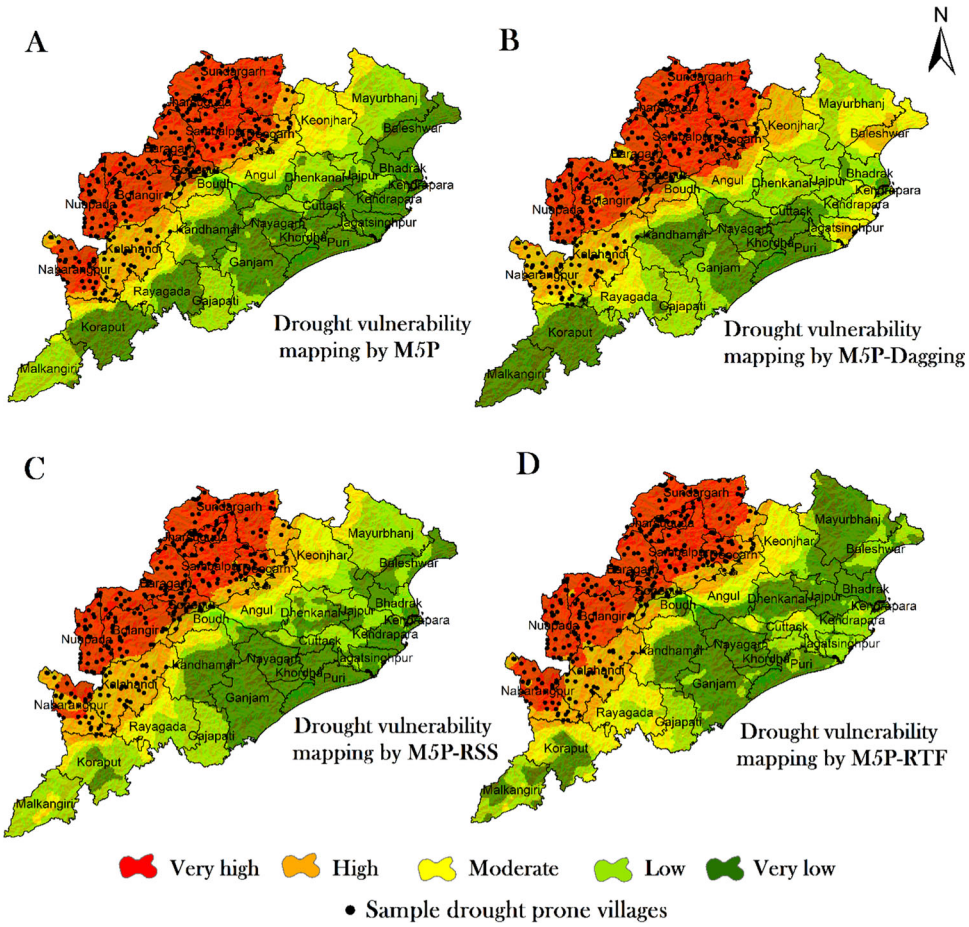


**Fig. 9** Drought vulnerability maps produced by: **A** M5P, **B** M5P-Dagging, **C** M5P-RSS, and **D** M5P-RTF

exposure, sensitivity and adaptive ability. To conduct this research, a wide variety of exposure, sensitivity and adaptive capacity factors were used to account for all possible drought scenarios. SPI-based drought estimation is well-established and has been utilised for the assessment of drought (Malik et al. 2020; Mehr et al. 2020). The criteria were chosen by depending on past studies and the geo-environmental conditions of the study area. The evaluation was conducted using well-known MLAs. Three ensemble models, namely, M5P-Dagging, M5P-RSS and M5P-RTF, were used for assessing drought vulnerability. Exposure, sensitivity and adaptive capacity maps were prepared by applying each of these ensemble models (M5P, M5P-Dagging, M5P-RSS and M5P-RTF) and by considering the indicators of exposure, sensitivity and adaptive capacity. A number of researchers used M5P, Dagging, RTF and RSS MLAs in numerous disciplines, such as predicting stream flow, (Onyari & Ilunga 2013), flood hazard (Nhu et al. 2020b), landslide (Antronico et al. 2020), assessment of deforestation susceptibility (Saha et al 2021b), gully erosion (Nhu et al. 2020a; Roy et al. 2021) and drought hazard (Buthelezi 2020). In each case, the capacity for forecasting of the output of the model was enormously appreciable. So, the use of the techniques of machine learning has become very frequent. However, these ensemble machine learning models have been used for assessing drought vulnerability. In other applications, such as landslides, floods, water level prediction and evaluation of the potential of spring, the M5P model has provided good output (Nhu et al. 2020a, b, c).

In the present research, all the applied models provided excellent results, as in the aforementioned fields. As compare to the conventional semi-quantitative method like AHP (Hoque et al. 2020; 2021) and Fuzzy-AHP (Saha et al 2021) the applied ensemble models provided better result in the present study. Among the applied models, M5P-RTF achieved the highest accuracy (90.10%). Among ensemble models, M5P was used as base classifier, and RSS, Dagging and RTF were used as meta classifiers. RSS and RTF increased the accuracy of the M5P base classifier. In the case of M5P-RTF ensemble model, the accuracy of the M5P base classifier was increased by nearly 5%, as the rotation forest is a tree-based ensemble that transforms the subsets of attributes before building each tree. When all of the attributes are real-valued, rotation forest outperformed the most frequent alternatives. In the present study better

**Table 8** Area under different drought vulnerability classes for every considered model

| Models | Vulnerability class | Area (%) | Area in (sq. km) |
|---|---|---|---|
| M5P | Very low | 32.25 | 50,227.39 |
| | Low | 19.71 | 30,702.20 |
| | Moderate | 12.41 | 19,324.03 |
| | High | 9.86 | 15,363.67 |
| | Very high | 25.74 | 40,089.71 |
| M5P—Dagging | Very low | 22.70 | 35,348.90 |
| | Low | 23.46 | 36,530.69 |
| | Moderate | 13.76 | 21,427.26 |
| | High | 14.94 | 23,271.19 |
| | Very high | 25.12 | 39,128.95 |
| M5P- RSS | Very low | 25.53 | 39,753.37 |
| | Low | 25.81 | 40,189.21 |
| | Moderate | 10.74 | 16,733.63 |
| | High | 14.22 | 22,156.45 |
| | Very high | 23.68 | 36,874.33 |
| M5P-RTF | Very low | 31.48 | 49,027.48 |
| | Low | 16.90 | 26,317.86 |
| | Moderate | 13.69 | 21,330.87 |
| | High | 12.34 | 19,227.12 |
| | Very high | 25.56 | 39,803.66 |

result of ensemble models has been found in case of M5P-RTF than other ensemble models applied in different fields like AdaBoost, Bagging, Dagging, MultiBoost, RTF, and RSS where ANN is base classifier in landslide modelling (Pham et al. 2017; Wang et al. 2020), staking and blending where KNN, RF and SVM were used as base classifiers in flood susceptibility modelling (Yao et al. 2022). This work's findings will undoubtedly aid in the formulation of drought relief measures in Odisha and will serve as a reference for future drought research, particularly in terms of strategy creation. Four maps – exposure, sensitivity, adaptive capability and drought vulnerability maps – were created, each of which was categorised into five groups using the natural break technique (Hoque et al. 2020; 2021). As per the categorisation, the state's north-western regions are extremely vulnerable to drought, owing to rising temperatures, declining rainfall, a high frequency of extreme drought, limited water supply, high evaporation and high water demand. The eastern half of the state is rather drought-resistant due to its location along the Bay of Bengal's coastal strip. It is important to raise awareness on the threat of drought in this region to protect the people who are dependent on agricultural activity. There is good scope for further elaboration of this work in future. New factors and indices can be added in the future to allow for a more exact depiction of drought vulnerability. Present day deep learning method have been used in different fields. In future deep learning method could be used for preparing the drought vulnerability maps. Drought-prediction techniques are improving over the time, and academics can keep up with them and improve them with their own contributions (Madrigal et al. 2018). With more ground level data, the models' accuracy can be improved even further. Such studies will help agricultural designers develop appropriate solutions in drought-prone areas.

### 4.1 Advantages of present work

Nevertheless, a full assessment of drought in the region requires the characterisation of drought, which permits activities such as early drought alarm and drought risk mitigation; this assessment would improve the preparation and catastrophe planning (Tsesmelis et al. 2019; Garca

**Table 9** Correlation between drought vulnerability and Exposure, Sensitivity and Adaptive capacity indices

| Indices | | Drought vulnerability index | | | |
|---|---|---|---|---|---|
| | | M5P -Dagging | M5P-RTF | M5P-RSS | M5P |
| Exposure | M5P-Dagging | .555 | .944 | .956 | .942 |
| | M5P-RTF | .561 | .995 | .991 | .982 |
| | M5P-RSS | .560 | .992 | .996 | .987 |
| | M5P | .545 | .990 | .993 | .990 |
| Sensitivity | M5P -Dagging | .556 | .971 | .963 | .956 |
| | M5P-RTF | .985 | .984 | .980 | .972 |
| | M5P-RSS | .661 | .983 | .981 | .973 |
| | M5P | .559 | .979 | .974 | .969 |
| Adaptive capacity | M5P -Dagging | .350 | .352 | .360 | .350 |
| | M5P-RTF | .448 | .562 | .463 | .457 |
| | M5P-RSS | .441 | .571 | .563 | .556 |
| | M5P | .426 | .528 | .427 | .494 |

**Table 10** Values of ROC and AUC

| Models | Area | Std. Error | Asymptotic Sig | Asymptotic 95% Confidence Interval | |
|---|---|---|---|---|---|
| | | | | Lower Bound | Upper Bound |
| *Training datasets* | | | | | |
| M5P -RTF | .873 | .063 | .000 | .750 | .995 |
| M5P -RSS | .855 | .059 | .000 | .739 | .971 |
| M5P | .842 | .060 | .000 | .724 | .960 |
| M5P -Dagging | .805 | .080 | .000 | .648 | .963 |
| *Testing datasets* | | | | | |
| M5P -RTF | .901 | .028 | .000 | .856 | .966 |
| M5P -RSS | .874 | .040 | .000 | .796 | .953 |
| M5P | .859 | .039 | .000 | .782 | .936 |
| M5P -Dagging | .852 | .039 | .000 | .775 | .929 |

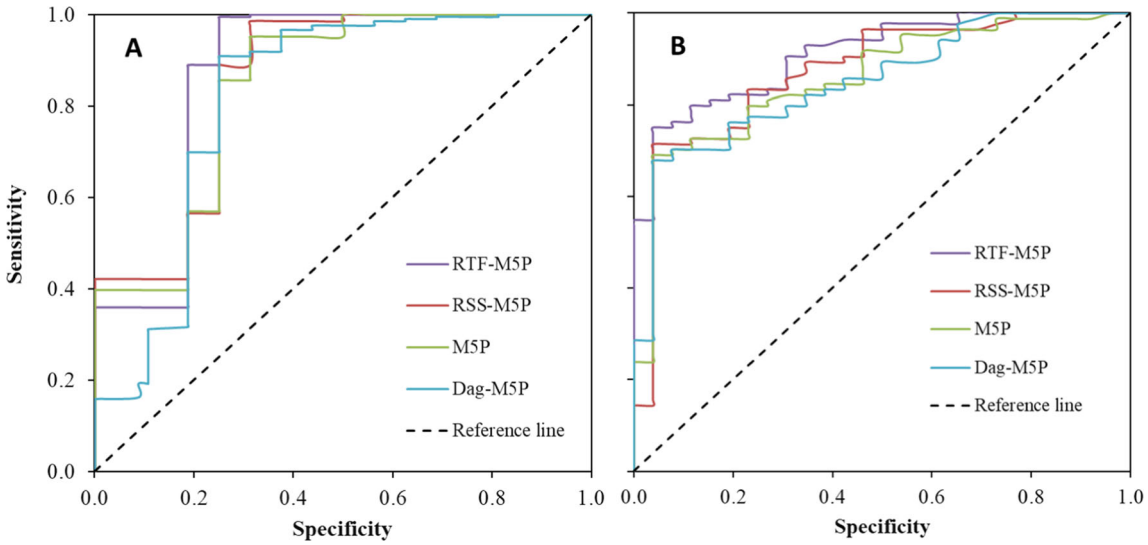


**Fig.10** ROC curves prepared for validating the applied using **A** training, and **B** testing datasets

**Table 11** Values of Precision, K- index, MAE and RMSE methods

| Model | Datasets | Precision | K- index | MAE | RMSE |
|---|---|---|---|---|---|
| M5P -RTF | Training | 0.873 | 0.879 | 0.269 | 0.146 |
| | Testing | 0.889 | 0.886 | 0.206 | 0.102 |
| M5P | Training | 0.813 | 0.801 | 0.382 | 0.228 |
| | Testing | 0.828 | 0.827 | 0.249 | 0.207 |
| M5P -RSS | Training | 0.836 | 0.814 | 0.241 | 0.174 |
| | Testing | 0.851 | 0.853 | 0.239 | 0.153 |
| M5P -Dagging | Training | 0.854 | 0.813 | 0.275 | 0.147 |
| | Testing | 0.868 | 0.856 | 0.253 | 0.139 |

**Table 12** : Friedman rank test result of drought vulnerability index

| Models | Mean Rank | Chi-Square | *P*-value | Significance |
|---|---|---|---|---|
| M5P | 2.47 | 11.936 | 0.007 | Yes |
| M5P-RSS | 2.56 | | | |
| M5P -RTF | 2.45 | | | |
| M5P -Dagging | 2.56 | | | |

et al. 2020). Our study provides a thorough analysis of the state's vulnerability to drought caused by a variety of factors. The first step in visualizing severely drought-stressed places is to use cartographic products like maps of drought susceptibility. Agricultural security has been identified as one of the most essential tools that farmers can use to protect themselves in the event of yield loss and to increase their adaptive ability (Akrofi-Atitianti et al. 2018). The farmers, irrigators, and block-level officials can use these maps to identify the region-specific causes of extreme drought vulnerability. Through capacity building, such information may aid in the effective planning of

**Table 13** Wilcoxon rank test result drought vulnerability index

| Models | Z-value | P-value | Significance |
|---|---|---|---|
| M5P Vs M5P -RSS | − 2.480[a] | 0.009 | Yes |
| M5P Vs M5P -RTF | − 2.753[a] | 0.005 | Yes |
| M5P Vs M5P -Dagging | − 2.244[a] | 0.011 | Yes |
| M5P -RTFVs M5P -RSS | − 2.478[b] | 0.013 | Yes |
| M5P -RSSVs M5P -Dagging | − 2.179[a] | 0.023 | Yes |
| M5P -RTFVs M5P -Dagging | − 2.634[a] | 0.008 | Yes |

agricultural operations and crop management strategies using the resources at hand. The created maps of drought vulnerability can help crop insurers to target regions that are vulnerable to drought and promote farmer involvement in crop insurance. Before moving further with the drought mitigation measures, the results of our study can also be complemented by the IMD's drought forecast maps. Additionally, the hydro-climate features, socioeconomic situation, or both in any location are realised from the bivariate choropleth maps as the dominating component driving the overall drought vulnerability. As a result, those involved in creating drought mitigation plans may want to think about strengthening drought-prone areas by improving their socioeconomic status and hydro-climatic adaptation. It is possible to improve the socio-economic situation through improving irrigation capacity, better groundwater conservation, and other measures. Contrarily, placing a focus on crop selection and appropriate agricultural management techniques with hydro-climatic condition can aid. In principle, the paradigm for assessing vulnerability to disasters described in this study may be employed to update drought vulnerability information with real-time data for adjustments to drought mitigation techniques.

## 5 Conclusion

In this research, for drought vulnerability evaluation, ensemble techniques have been adopted and implemented in Odisha, which has never been done before in drought vulnerability assessments. Considering that the nature of drought changes, the approaches for measuring drought susceptibility across place and time need to change as well. Fifty-three drought determining variables were layered on a GIS environment to create drought vulnerability maps based on prior studies. The M5P, M5P-Dagging, M5P-RSS and M5P-RTF ensemble models were combined with these factor layers. The M5P, M5P-Dagging, M5P-RSS and M5P-RTF ensemble models showed very-high drought vulnerability rates of 25.74%, 25.12%, 23.68% and 25.56% in the region, respectively. If effective drought management strategies are not adopted, then this area would undoubtedly be susceptible in the near future. We could not conduct field observations and document the perception of local people due to fund and time deficits. However, such a flaw has no bearing on the used models' correctness. The state's northern areas are particularly vulnerable to drought due to increasing temperatures, diminishing rainfall, a high frequency of extreme drought, restricted water supply, high evaporation and high water demand. The eastern half of the state is drought-resistant due to its location along the Bay of Bengal's coastal strip. The main limitations of the study include lack of crop type data pr agricultural practices in the drought vulnerable region. Future research may focus on the impact of drought vulnerability on agriculture and socio-economic conditions as well as how drought vulnerability evolves under the changing climate and socio-economic conditions. However, the government should implement a variety of programmes and increase public awareness. Odisha could construct various machinery and irrigational infrastructures to aid in water conservation. The findings of this study can be utilised through local government and private organisations in the Indian state of Odisha for the management of water resource, preservation of environment and land use planning.

## 6 author Contributions statement

SS: Methodology, Format analysis, Supervision, Writing original draft preparation; Writing review and editing, BK: Methodology, Format analysis, investigation, software, writing original draft preparation, Gopal CP: Methodology, Format analysis, investigation, software, writing original draft preparation; BP: Visualisation, Extensive writing review and editing.

**Author contributions** Methodology by S.S and G.C.P; Format analysis by S.S, B.K and G.C.P; Writing original draft preparation by S.S, B.K and G.C.P; Writing review and editing by S.S, G.C.P and B.P; Visualization by S.S, B.K, G.C.P and B.P; Figures by S.S, B.K and G.C.P investigation by B.K and G.C.P; Data collected by B.K and G.C.P.

**Funding** Open Access funding enabled and organized by CAUL and its Member Institutions. No fund was received for this work.

### Declarations

**Competing interests** The authors declare no competing interests.

**Conflict of Interest** None.

## References

Abbas S, Kousar S (2021) Spatial analysis of drought severity and magnitude using the standardized precipitation index and streamflow drought index over the Upper Indus Basin, Pakistan. Environ Dev Sustain 23(10):15314–15340

Ajayi VO, Ilori OW (2020) Projected drought events over West Africa using RCA4 regional climate model. Earth Systems Environ 4(2):329–348

Akrofi-Atitianti F, IfejikaSperanza C, Bockel L, Asare R (2018) Assessing climate smart agriculture and its determinants of practice in Ghana: a case of the cocoa production system. Land 7(1):30

Alodah A. (2019). Stochastic assessment of climate-induced risk for water resources systems in a bottom-up framework (Doctoral dissertation, Universitéd'Ottawa/University of Ottawa).

Amrit K, Pandey RP, Mishra SK (2018) Characteristics of meteorological droughts in northwestern India. Nat Hazards 94(2):561–582

Antronico L, De Pascale F, Coscarelli R, Gullà G (2020) Landslide risk perception, social vulnerability and community resilience: the case study of Maierato (Calabria, southern Italy). Int J Disaster Risk Reduct 46:101529

Baarsch F, Granadillos JR, Hare W, Knaus M, Krapp M, Schaeffer M, Lotze-Campen H (2020) The impact of climate change on incomes and convergence in Africa. World Dev 126:104699

Bakht S, Safdar K, Khair K U, Fatima A, Fayyaz, A., Ali, S. M., Munir, H., Farid, M., 2020. The Response of Major Food Crops to Drought Stress: Physiological and Biochemical Responses. In Agronomic Crops (pp. 93–115). Springer, Singapore.

Balaganesh G, Malhotra R, Sendhil R, Sirohi S, Maiti S, Ponnusamy K, Sharma AK (2020) Development of composite vulnerability index and district level mapping of climate change induced drought in Tamil Nadu. India Ecol Indicat 113:106197

Banihashemi SM, Eslamian SS, Nazari B (2021) The impact of climate change on wheat, barley, and maize growth indices in near-future and far-future periods in Qazvin Plain. Iran International Journal of Plant Production 15(1):45–60

Barzegar R, Razzagh S, Quilty J, Adamowski J, Pour HK, Booij MJ (2021) Improving GALDIT-based groundwater vulnerability predictive mapping using coupled resampling algorithms and machine learning models. J Hydrol 598:126370

Belesova K, Agabiirwe CN, Zou M, Phalkey R, Wilkinson P (2019) Drought exposure as a risk factor for child undernutrition in low- and middle-income countries: A systematic review and assessment of empirical evidence. Environ Int 131:104973

Bevacqua A, Yu D, Zhang Y (2018) Coastal vulnerability: Evolving concepts in understanding vulnerable people and places. Environ Sci Policy 82:19–29

Brahmachari K, Sarkar S, Santra DK, Maitra S (2019) Millet for food and nutritional security in drought prone and red laterite region of Eastern India. Int J Plant Soil Sci 26(6):1–7

Buthelezi M. N. M, (2020) The use of machine learning algorithms to assess the impacts of droughts on commercial forests in KwaZulu-Natal, South Africa (Doctoral dissertation).

Cao S, He Y, Zhang L, Chen Y, Yang W, Yao S, Sun Q (2021) Spatiotemporal characteristics of drought and its impact on vegetation in the vegetation region of Northwest China. Ecol Ind 133:108420

Chai Y, Li Y, Yang Y, Li S, Zhang W, Ren J, Xiong H (2019) Water level variation characteristics under the impacts of extreme drought and the operation of the three Gorges Dam. Frontiers of Earth Science 13(3):510–522

Chung CR, Wang HY, Lien F, Tseng YJ, Chen CH, Lee TY, Liu PT, Horng JT, Lu JJ (2019) Incorporating statistical test and machine intelligence into strain typing of Staphylococcus haemolyticus based on matrix-assisted laser desorption ionization-time of flight mass spectrometry. Front Microbiol 10:2120

Cianconi P, Betrò S, Janiri L (2020) The impact of climate change on mental health: a systematic descriptive review. Front Psych 11:74

Costello FJ, Lee KC (2020) Exploring the Sentiment Analysis of Electric Vehicles Social Media Data by Using Feature Selection Methods. J Digital Converg 18(2):249–259

da Rocha Júnior RL, dos Santos Silva FD, Costa RL, Gomes HB, Pinto DDC, Herdies DL (2020) Bivariate assessment of drought return periods and frequency in brazilian northeast using joint distribution by copula method. Geosciences 10(4):135

Dai A, Zhao T, Chen J (2018) Climate change and drought: a precipitation and evaporation perspective. Current Clim Change Rep 4(3):301–312

Dar MH, Waza SA, Shukla S, Zaidi NW, Nayak S, Hossain M, Singh US (2020) Drought tolerant rice for ensuring food security in Eastern India. Sustainability 12(6):2214

Datta PS (2019) Water harvesting for groundwater management: issues, perspectives, scope, and challenges. John Wiley & Sons

Dayal KS, Deo RC, Apan AA (2018) Investigating drought duration-severity-intensity characteristics using the Standardized Precipitation-Evapotranspiration Index: case studies in drought-prone Southeast Queensland. J Hydrol Eng 23(1):05017029

Dikshit A, Pradhan B, Alamri AM (2020) Pathways and challenges of the application of artificial intelligence to geohazards modelling. Gondwana Res. https://doi.org/10.1016/j.gr.2020.08.007

Dikshit A, Pradhan B, Huete A (2021a) An improved SPEI drought forecasting approach using the long short-term memory neural network. J Environ Manag 283:111979. https://doi.org/10.1016/j.jenvman.2021.111979

Dikshit A, Pradhan B (2021b) Interpretable and explainable AI (XAI) model for spatial drought prediction. Sci Total Environ 801:149797. https://doi.org/10.1016/j.scitotenv.2021.149797

Ebi K, Kovats RS, Menne B (2006) An approach for assessing human health vulnerability and public health interventions to adapt to climate change. Environ Health Perspect 114:1930–1934

Ekwueme BN, Agunwamba JC (2020) Modeling the influence of meteorological variables on runoff in a tropical watershed. Civil Eng J 6(12):2344–2351

Ety NJ, Chu Z, Masum SM (2021) Monitoring of flood water propagation based on microwave and optical imagery. Quatern Int 574:137–145

Fadhil AM (2011) Drought mapping using Geoinformation technology for some sites in the Iraqi Kurdistan region. Int Journal of Digital Earth 4(3):239–257

Feng P, Liu DL, Wang B, Waters C, Zhang M, Yu Q (2019a) Projected changes in drought across the wheat belt of

southeastern Australia using a downscaled climate ensemble. Int J Climatol 39(2):1041–1053
Feng P, Wang B, Li Liu D, Yu Q (2019b) Machine learning-based integration of remotely-sensed drought factors can improve the estimation of agricultural drought in South-Eastern Australia. Agric Syst 173:303–316
Freund Y, Schapire RE (1997) A desicion-theoretic generalization of on-line learning and an application to boosting. J Comput Syst Sci 55:119–139
García W. C. A. C., Boccardo P. (2020) Vegetation Dynamics and Their Relationships with Precipitation in Africa for Drought Monitoring Purposes.
GeranMalek A, Mansoori M, Omranpour H (2021) Random forest and rotation forest ensemble methods for classification of epileptic EEG signals based on improved 1D-LBP feature extraction. Int J Imaging Syst Technol 31(1):189–203
Germain C., Knight C (2021) 2 The Ecological Perspective. In The life model of social work practice (pp. 54–81). Columbia University Press.
Ghada W, Estrella N, Menzel A (2019) Machine learning approach to classify rain type based on Thiesdisdrometers and cloud observations. Atmosphere 10(5):251
Guo H, Wang R, Garfin GM, Zhang A, Lin D (2021) Rice drought risk assessment under climate change: Based on physical vulnerability a quantitative assessment method. Sci Total Environ 751:141481
Haile GG, Tang Q, Li W, Liu X, Zhang X (2020) Drought: Progress in broadening its understanding. Wiley Interdiscip Rev Water 7(2):e1407
Han L, Zhang Q, (2018) August. research progress on the agriculture drought disaster risk and its research theoretical framework. In 2018 7th International Conference on Agro-geoinformatics (Agro-geoinformatics) (pp. 1–4). IEEE.
Helcoski R, Yonkos LT, Sanchez A, Baldwin AH (2020) Wetland soil microplastics are negatively related to vegetation cover and stem density. Environ Pollut 256:113391
Heldt FS, Vizcaychipi MP, Peacock S, Cinelli M, McLachlan L, Andreotti F, Jovanovic S, Durichen R, Lipunova N, Fletcher RA, Hancock A, McCarthy A, Pointon RA, Brown A, Eaton J, Liddi R, Mackillop L, Tarassenko L, Khan RT (2021) Early risk assessment for COVID-19 patients from emergency department data using machine learning. Sci Rep 11(1):1–13
Hong QN, Gonzalez-Reyes A, Pluye P (2018) Improving the usefulness of a tool for appraising the quality of qualitative, quantitative and mixed methods studies, the Mixed Methods Appraisal Tool (MMAT). J Eval Clin Pract 24(3):459–467
Hoque MAA, Pradhan B, Ahmed N (2020) Assessing drought vulnerability using geospatial techniques in northwestern part of Bangladesh. Sci Total Environ 705:135957
Hoque MAA, Pradhan B, Ahmed N, Sohel MSI (2021) Agricultural drought risk assessment of Northern New South Wales, Australia using geospatial techniques. Sci Total Environ 756:143600
Hribar MR, Read-Brown S, Goldstein IH, Reznick LG, Lombardi L, Parikh M, Chamberlin W, Chiang MF (2018) Secondary use of electronic health record data for clinical workflow analysis. J Am Med Inform Assoc 25(1):40–46
Hurlbert MA, Gupta J (2019) An institutional analysis method for identifying policy instruments facilitating the adaptive governance of drought. Environ Sci Policy 93:221–231
Huynh LTM, Stringer LC (2018) Multi-scale assessment of social vulnerability to climate change: An empirical study in coastal Vietnam. Clim Risk Manag 20:165–180
Intergovernmental Panel on Climate Change (IPCC), 2001, Climate change 2001: Impacts, adaptation, and vulnerability, Cambridge University Press, Cambridge
Islam MZ, Saha T, Monalisa K, Hoque MM (2019) Effect of starch edible coating on drying characteristics and antioxidant properties of papaya. J Food Measure Character 13(4):2951–2960
Javadinejad S, Dara R, Jafary F (2020) Analysis and prioritization the effective factors on increasing farmers resilience under climate change and drought. Agricul Res. https://doi.org/10.1007/s40003-020-00516-w
Jiang W, Wang L, Zhang M, Yao R, Chen X, Gui X, Cao Q (2021) Analysis of drought events and their impacts on vegetation productivity based on the integrated surface drought index in the Hanjiang River Basin. China. Atmospheric Res 254:105536
Karimi V, Karami E, Keshavarz M (2018) Climate change and agriculture: Impacts and adaptive responses in Iran. J Integr Agric 17(1):1–15
Karstoft KI, Nielsen T, Nielsen AB (2021) Measuring social support among soldiers with the experienced Post-deployment Social Support Scale (EPSSS): a Rasch-based construct validity study. Behav Med 47(2):131–139
Kaufman SB, Weiss B, Miller JD, Campbell WK (2020) Clinical correlates of vulnerable and grandiose narcissism: a personality perspective. J Pers Disord 34(1):107–130
Kobrossi J, Karam F, Mitri G (2021) Rain pattern analysis using the Standardized Precipitation Index for long-term drought characterization in Lebanon. Arab J Geosci 14(1):1–17
Liang L (2014) Drought change trend using MODIS TVDI and its relationship with climate factors in China from 2001 to 2010. J Integr Agric 13(7):1501–1508
Lin H, Wang J, Li F, Xie Y, Jiang C, Sun L (2020) Drought trends and the extreme drought frequency and characteristics under climate change based on SPI and HI in the upper and middle reaches of the Huai River Basin. China Water 12(4):1100
Liu L, Yang X, Zhou H, Liu S, Zhou L, Li X, Wu J (2018) Evaluating the utility of solar-induced chlorophyll fluorescence for drought monitoring by comparison with NDVI derived from wheat canopy. Sci Total Environ 625:1208–1217
Machado-Silva F, Libonati R, de Lima TFM, Peixoto RB, de Almeida Franca JR, Magalhães MDAFM, DaCamara CC (2020) Drought and fires influence the respiratory diseases hospitalizations in the Amazon. Ecol Indcators 109:105817
Madrigal J, Solera A, Suárez-Almiñana S, Paredes-Arquiola J, Andreu J, Sánchez-Quispe ST (2018) Skill assessment of a seasonal forecast model to predict drought events for water resource systems. J Hydrol 564:574–587
Mafi-Gholami D, Zenner EK, Jaafari A (2020) Mangrove regional feedback to sea level rise and drought intensity at the end of the 21st century. Ecol Ind 110:105972
Malik A, Kumar A, Salih SQ, Kim S, Kim NW, Yaseen ZM, Singh VP (2020) Drought index prediction using advanced fuzzy logic model: Regional case study over Kumaon in India. PLoS ONE 15(5):e0233280
Marusig D, Petruzzellis F, Tomasella M, Napolitano R, Altobelli A, Nardini A (2020) Correlation of field-measured and remotely sensed plant water status as a tool to monitor the risk of drought-induced forest decline. Forests 11(1):77
Masanta SK, Srinivas VV (2022) Proposal and evaluation of nonstationary versions of SPEI and SDDI based on climate covariates for regional drought analysis. J Hydrol. https://doi.org/10.1016/j.jhydrol.2022.127808
Mbiriri, M., Mukwada, G., & Manatsa, D. (2018). Influence of altitude on the spatiotemporal variations of meteorological droughts in mountain regions of the free state Province, South Africa (1960–2013). Advances in Meteorology, 2018.
McCune JL, Rosner-Katz H, Bennett JR, Schuster R, Kharouba HM (2020) Do traits of plant species predict the efficacy of species distribution models for finding new occurrences? Ecol Evol 10(11):5001–5014

McKee TB, Doesken NJ, Kleist J. 1993. The relationship of drought frequency and duration to time scales. Eighth Conference on Applied Climatology. Boston, MA: American Meteorological Society.

Mega R, Abe F, Kim JS, Tsuboi Y, Tanaka K, Kobayashi H, Sakata Y, Hanada K, Tsujimoto H, Kikuchi J, Cutler SR, Okamoto M, Okamoto M (2019) Tuning water-use efficiency and drought tolerance in wheat using abscisic acid receptors. Nature Plants 5(2):153–159

Mehdipour S, Nakhaee N, Zolala F, Okhovati M, Foroud A, Haghdoost AA (2022) A systematized review exploring the map of publications on the health impacts of drought. Nat Hazards. https://doi.org/10.1007/s11069-022-05311-0

Mehr AD, Vaheddoost B, Mohammadi B (2020) ENN-SA: A novel neuro-annealing model for multi-station drought prediction. Comput Geosci 145:104622

Meza I, Siebert S, Döll P, Kusche J, Herbert C, Eyshi Rezaei E, Hagenlocher M (2020) Global-scale drought risk assessment for agricultural systems. Nat Hazards Earth Syst Sci 20(2):695–712

Miraki S, Zanganeh SH, Chapi K, Singh VP, Shirzadi A, Shahabi H, Pham BT (2019) Mapping groundwater potential using a novel hybrid intelligence approach. Water Resour Manage 33(1):281–302

Mirgol B, Nazari M, Etedali HR, Zamanian K (2021) Past and future drought trends, duration, and frequency in the semi-arid Urmia Lake Basin under a changing climate. Meteorol Appl 28(4):e2009

Mishra A, Bruno E, Zilberman D (2021) Compound natural and human disasters: Managing drought and COVID-19 to sustain global agriculture and food sectors. Sci Total Environ 754:142210

Moser P, Simon MF, de Medeiros MB, Gontijo AB, Costa FRC (2019) Interaction between extreme weather events and mega-dams increases tree mortality and alters functional status of Amazonian forests. J Appl Ecol 56(12):2641–2651

Mukherjee N, Siddique G, Basak A, Roy A, Mandal MH (2019) Climate change and livelihood vulnerability of the local population on Sagar Island. India Chinese Geographical Science 29(3):417–436

Murthy, R. V. R., 2020. Mapping Spatio-Temporal Cropland Changes Due To Water Stress in Krishna River Basin Using Temporal Satellite Data (Doctoral dissertation, College of Engineering (A), Andhra University, Visakhapatnam).

Nabaei S, Sharafati A, Yaseen ZM, Shahid S (2019) Copula based assessment of meteorological drought characteristics: regional investigation of Iran. Agric for Meteorol 276:107611

Nabipour N, Dehghani M, Mosavi A, Shamshirband S (2020) Short-term hydrological drought forecasting based on different nature-inspired optimization algorithms hybridized with artificial neural networks. IEEE Access 8:15210–15222

Nanzad L, Zhang J, Tuvdendorj B, Nabil M, Zhang S, Bai Y (2019) NDVI anomaly for drought monitoring and its correlation with climate factors over Mongolia from 2000 to 2016. J Arid Environ 164:69–77

Nasrollahi M, Khosravi H, Moghaddamnia A, Malekian A, Shahid S (2018) Assessment of drought risk index using drought hazard and vulnerability indices. Arab J Geosci 11(20):1–12

Naumann G, Vargas WM, Barbosa P, Blauhut V, Spinoni J, Vogt JV (2019) Dynamics of socioeconomic exposure, vulnerability and impacts of recent droughts in Argentina. Geosciences 9(1):39

Nhu VH, Janizadeh S, Avand M, Chen W, Farzin M, Omidvar E, Shirzadi A, Shahabi H, Clague JJ, Jaafari A, Mansoorypoor F, Pham BT, Ahamad BB, Lee S (2020a) Gis-based gully erosion susceptibility mapping: A comparison of computational ensemble data mining models. Appl Sci 10(6):2039

Nhu VH, Shahabi H, Nohani E, Shirzadi A, Al-Ansari N, Bahrami S, Miraki S, Geertsema M, Nguyen H (2020b) Daily Water Level Prediction of Zrebar Lake (Iran): A Comparison between M5P, Random Forest, Random Tree and Reduced Error Pruning Trees Algorithms. ISPRS Int J Geo Inf 9(8):479

Nhu VH, Thi Ngo PT, Pham TD, Dou J, Song X, Hoang ND, Tran DA, Cao DP, Aydilek LB, Amiri M, Costache R, Hoe PV, Tien Bui D (2020c) A new hybrid firefly–PSO optimized random subspace tree intelligence for torrential rainfall-induced flash flood susceptible mapping. Remote Sensing 12(17):2688

Nguyen PT, Ha DH, Jaafari A, Nguyen HD, Van Phong T, Al-Ansari N, Prakash I, Le HV, Pham BT (2020) Groundwater potential mapping combining artificial neural network and real AdaBoost ensemble technique: the DakNong province case-study. Vietnam. Int J Environ Res Publ Health 17(7):2473

Nübler L, Austrian K, Maluccio JA, Pinchoff J (2021) Rainfall shocks, cognitive development and educational attainment among adolescents in a drought-prone region in Kenya. Environ Dev Econ 26(5–6):466–487

Nyairo R, Machimura T, Matsui T (2020) A combined analysis of sociological and farm management factors affecting household livelihood vulnerability to climate change in rural burundi. Sustainability 12(10):4296

Ogunrinde AT, Oguntunde PG, Akinwumiju AS, Fasinmirin JT (2019) Analysis of recent changes in rainfall and drought indices in Nigeria, 1981–2015. Hydrol Sci J 64(14):1755–1768

Onyari EK, Ilunga FM (2013) Application of MLP neural network and M5P model tree in predicting streamflow: A case study of Luvuvhu catchment, South Africa. Int J Innovat, Manage Technol 4(1):11

Ortiz-Bobea, A., 2021. Climate, Agriculture and Food. *arXiv preprint* arXiv:2105.12044.

Ouatiki H, Boudhar A, Ouhinou A, Arioua A, Hssaisoune M, Bouamri H, Benabdelouahab T (2019) Trend analysis of rainfall and drought over the Oum Er-Rbia River Basin in Morocco during 1970–2010. Arab J Geosci 12(4):1–11

Panda A, Sahu N (2019) Trend analysis of seasonal rainfall and temperature pattern in Kalahandi, Bolangir and Koraput districts of Odisha. India Atmosph Sci Lett 20(10):e932

Patel KF, Fansler SJ, Campbell TP, Bond-Lamberty B, Smith AP, RoyChowdhury T, Bailey VL (2021) Soil texture and environmental conditions influence the biogeochemical responses of soils to drought and flooding. Communicat Earth Environ 2(1):1–9

Paul M, Negahban-Azar M, Shirmohammadi A, Montas H (2020) Assessment of agricultural land suitability for irrigation with reclaimed water using geospatial multi-criteria decision analysis. Agric Water Manag 231:105987

Payab AH, Türker U (2018) Analyzing temporal–spatial characteristics of drought events in the northern part of Cyprus. Environ Dev Sustain 20(4):1553–1574

Pham BT, Bui DT, Prakash I, Dholakia MB (2017) Hybrid integration of Multilayer Perceptron Neural Networks and machine learning ensembles for landslide susceptibility assessment at Himalayan area (India) using GIS. CATENA 149:52–63

Phelps D, Kelly D (2019) Overcoming drought vulnerability in rangeland communities: lessons from central-western Queensland. The Rangeland Journal 41(3):251–270

Pidathala, S., Dhiman, S., Patra, K. C., 2018. Management of Flood and Drought through Development of Water Resources in Odisha State.

Potopová V, Lhotka O, Možný M, Musiolková M (2021) Vulnerability of shop -yields due to compound drought and heat events over European key s-hop regions. Int J Climatol 41:E2136–E2158

Rahman G, Dawood M (2018) Spatial and temporal variation of rainfall and drought in Khyber Pakhtunkhwa Province of Pakistan during 1971–2015. Arab J Geosci 11(3):1–13

Reynolds, C. R., Altmann, R. A., Allen, D. N., 2021. The problem of bias in psychological assessment. In Mastering Modern Psychological Testing (pp. 573–613). Springer, Cham.

Rosselló J, Becken S, Santana-Gallego M (2020) The effects of natural disasters on international tourism: A global analysis. Tour Manage 79:104080

Roy J, Saha S (2021) Integration of artificial intelligence with meta classifiers for the gully erosion susceptibility assessment in Hinglo river basin. Eastern India Adv Space Res 67(1):316–333

Sahu PC, Nandi D (2016) Groundwater resource estimation and budgeting for sustainable growth in agriculture in a part of drought prone Sundergarh district, Odisha, India. Int Res J Earth Sci 4(2):9–14

Saha S, Kundu B, Paul GC, Mukherjee K, Pradhan B, Dikshit A, Maulud KNA, Alamri AM (2021a) Spatial assessment of drought vulnerability using fuzzy-analytical hierarchical process: a case study at the Indian state of Odisha. Geomat Nat Haz Risk 12(1):123–153

Saha S, Paul GC, Pradhan B, Abdul Maulud KN, Alamri AM (2021b) Integrating multilayer perceptron neural nets with hybrid ensemble classifiers for deforestation probability assessment in Eastern India. Geomat Nat Haz Risk 12(1):29–62

Saha S, Gogoi P, Gayen A, Paul GC (2021c) Constructing the machine learning techniques based spatial drought vulnerability index in Karnataka state of India. J Cleaner Prod 128073

Salih SQ, Sharafati A, Khosravi K, Faris H, Kisi O, Tao H, Ali M, Yaseen ZM (2020) River suspended sediment load prediction based on river discharge information: Application of newly developed data mining models. Hydrol Sci J 65(4):624–637

Sam AS, Padmaja SS, Kächele H, Kumar R, Müller K (2020) Climate change, drought and rural communities: Understanding people's perceptions and adaptations in rural eastern India. International J of Disaster Risk Reduct 44:101436

Sankaran M (2019) Droughts and the ecological future of tropical savanna vegetation. J Ecol 107(4):1531–1549

Santos CAG, Neto RMB (2021) Geospatial drought severity analysis based on PERSIANN-CDR-estimated rainfall data for Odisha state in India (1983–2018). Sci Total Environ 750:141258

Senapati AK (2019) An indicator-based approach to assess farm households' vulnerability to climate change: evidence from Odisha. India Spatial Inform Res. https://doi.org/10.1007/s41324-019-00277-x

Seni G, Elder JF (2010) Ensemble methods in data mining: improving accuracy through combining predictions. Synthesis Lectures on Data Mining Knowl Discovery 2(1):1–126

Sharafi L, Zarafshani K, Keshavarz M, Azadi H, Van Passel S (2020) Drought risk assessment: towards drought early warning system and sustainable environment in western Iran. Ecol Ind 114:106276

Sharma TC, Panu US (2021) A drought magnitude-based method for reservoir sizing: A case of annual and monthly flows from Canadian rivers. J Hydrol: Regional Studies 36:100829

Shashikant V, Mohamed Shariff AR, Wayayok A, Kamal MR, Lee YP, Takeuchi W (2021) Utilizing TVDI and NDWI to Classify Severity of Agricultural Drought in Chuping. Malaysia Agronomy 11(6):1243

Shi W, Huang S, Liu D, Huang Q, Han Z, Leng G, Wang H, Liang H, Li P, Wei X (2021) Drought-flood abrupt alternation dynamics and their potential driving forces in a changing environment. J Hydrol 597:126179

Silva I, Eugenio Naranjo J (2020) A systematic methodology to evaluate prediction models for driving style classification. Sensors 20(6):1692

Singha P, Das P, Talukdar S, Pal S (2020) Modeling livelihood vulnerability in erosion and flooding induced river island in Ganges riparian corridor. India Ecol Indicat 119:106825

Stirling E, Fitzpatrick RW, Mosley LM (2020) Drought effects on wet soils in inland wetlands and peatlands. Earth Sci Rev 210:103387

Subasi A, Ahmed A, Aličković E, Hassan AR (2019) Effect of photic stimulation for migraine detection using random forest and discrete wavelet transform. Biomed Signal Process Control 49:231–239

Sun F, Mejia A, Zeng P, Che Y (2019) Projecting meteorological, hydrological and agricultural droughts for the Yangtze River basin. Sci Total Environ 696:134076

Swain S, Mishra SK, Pandey A (2021a) A detailed assessment of meteorological drought characteristics using simplified rainfall index over Narmada River Basin. India Environmental Earth Sciences 80(6):1–15

Swain S, Mishra SK, Pandey A, Kalura P (2022) Inclusion of groundwater and socio-economic factors for assessing comprehensive drought vulnerability over Narmada River Basin, India: A geospatial approach. Appl Water Sci 12(2):1–16

Swain, S., Mishra, S. K., Pandey, A., Dayal, D., (2021b) Identification of meteorological extreme years over central division of Odisha using an index-based approach. In *Hydrological Extremes* (pp. 161–174). Springer, Cham.

Talukdar S, Ghose B, Salam R, Mahato S, Pham QB, Linh NTT, Costache R, Avand M (2020) Flood susceptibility modeling in Teesta River basin, Bangladesh using novel ensembles of bagging algorithms. Stoch Env Res Risk Assess 34(12):2277–2300

Thomas T, Jaiswal RK, Galkate R, Nayak PC, Ghosh NC (2016) Drought indicators-based integrated assessment of drought vulnerability: a case study of Bundelkhand droughts in central India. Nat Hazards 81(3):1627–1652

Tien Bui D, Pham BT, Nguyen QP, Hoang ND (2016) Spatial prediction of rainfall-induced shallow landslides using hybrid integration approach of Least-Squares Support Vector Machines and differential evolution optimization: a case study in Central Vietnam. Int J Digital Earth 9(11):1077–1097

Tien Bui D, Shahabi H, Shirzadi A, Chapi K, Pradhan B, Chen W, Khosravi K, Panahi M, Ahmad BB, Saro L (2018) Land subsidence susceptibility mapping in South Korea using machine learning algorithms. Sensors 18(8):2464

Tsesmelis DE, Oikonomou PD, Vasilakou CG, Skondras NA, Fassouli V, Alexandris SG, Grigg NS, Karavitis CA (2019) Assessing structural uncertainty caused by different weighting methods on the Standardized Drought Vulnerability Index (SDVI). Stoch Env Res Risk Assess 33(2):515–533

Tsiros IX, Nastos P, Proutsos ND, Tsaousidis A (2020) Variability of the aridity index and related drought parameters in Greece using climatological data over the last century (1900–1997). Atmos Res 240:104914

Turner, B. S. (2021). Vulnerability and human rights. Penn State University Press.

Ullah H, Santiago-Arenas R, Ferdous Z, Attia A, Datta A (2019) Improving water use efficiency, nitrogen use efficiency, and radiation use efficiency in field crops under drought stress: A review. Adv Agron 156:109–157

Ünlü R (2020) An assessment of machine learning models for slump flow and examining redundant features. Comput Concr 25(6):565–574

Venancio LP, Filgueiras R, Mantovani EC (2020) Impact of drought associated with high temperatures on Coffeacanephora plantations: a case study in Espírito Santo State. Brazil Scientific Reports 10(1):1–21

Wable PS, Jha MK, Shekhar A (2019) Comparison of drought indices in a semi-arid river basin of India. Water Resour Manage 33(1):75–102

Wang Y, Feng L, Li S, Ren F, Du Q (2020) A hybrid model considering spatial heterogeneity for landslide susceptibility mapping in Zhejiang Province. China Catena 188:104425

West H, Quinn N, Horswell M (2019) Remote sensing for drought monitoring & impact assessment: Progress, past challenges and future opportunities. Remote Sens Environ 232:111291

Willmott CJ, Matsuura K (2005) Advantages of the mean absolute error (MAE) over the root mean square error (RMSE) in assessing average model performance. Clim. Res. 30(1):79–82

Wolpert DH (1992) Stacked generalization. Neural Netw 5(2):241–259. https://doi.org/10.1016/S0893-6080(05)80023-1

Wu G, Guan K, Li Y, Novick KA, Feng X, McDowell NG, Konings AG, Thompson SE, Kimbal JS, Kauwe MG, Ainsworth NA, Jiang C (2021) Interannual variability of ecosystem iso/anisohydry is regulated by environmental dryness. New Phytol 229(5):2562–2575

Yao J, Zhang X, Luo W, Liu C, Ren L (2022) Applications of Stacking/Blending ensemble learning approaches for evaluating flash flood susceptibility. Int J Appl Earth Obs Geoinf 112:102932

Yu H, Zhang Q, Sun P, Song C (2018) Impact of droughts on winter wheat yield in different growth stages during 2001–2016 in Eastern China. Int J Disaster Risk Sci 9(3):376–391

Yves T, Koutroulis A, Samaniego L, Vicente-Serrano SM, Volaire F, Boone A, Page ML, Liasat MC Albergel C, Burak S, Cailleret M, Kalin KC, Davi H, Dupuy JL, Greve P, Grillakis M, Hanich L, Jarlan L, St Paul NM, Vilalta JM, Mouillot F, Velazquez DP, Segui PQ, Renard D, Turkes M, Trigo R, Vidal JP, Vilagrosa A, Zribi M, Polcher J (2020) Challenges for drought assessment in the Mediterranean region under future climate scenarios. Earth-Sci Rev 103348.

Zahraie B, Nasseri M (2011) Basin scale meteorological drought forecasting using support vector machine (SVM). In: International conference on drought management strategies in arid and semi arid regions. Muscat, Oman (pp 1–16)

Zhang M, He J, Wang B, Wang S, Li S, Liu W, Ma X (2013) Extreme drought changes in Southwest China from 1960 to 2009. J Geog Sci 23(1):3–16

Zhang G, Zhao W, Zhou H, Yang Q, Wang X (2018) Extreme drought stress shifts net facilitation to neutral interactions between shrubs and sub-canopy plants in an arid desert. Oikos 127(3):381–391

Zhang B, AghaKouchak A, Yang Y, Wei J, Wang G (2019) A water-energy balance approach for multi-category drought assessment across globally diverse hydrological basins. Agric for Meteorol 264:247–265

Zhang F, Biederman JA, Dannenberg MP, Yan D, Reed SC, Smith WK (2021) Five decades of observed daily precipitation reveal longer and more variable drought events across much of the western United States. Geophys Res Lett 48(7):e2020GL092293

Zhang R, Wu X, Zhou X, Ren B, Zeng J, Wang Q (2022) Investigating the effect of improved drought events extraction method on spatiotemporal characteristics of drought. Theoret Appl Climatol 147(1):395–408

Zounemat-Kermani M, Batelaan O, Fadaee M, Hinkelmann R (2021) Ensemble machine learning paradigms in hydrology: a review. J Hydrol 598:126266



## Authors and Affiliations

**Sunil Saha[1] · Barnali Kundu[1] · Gopal Chandra Paul[1] · Biswajeet Pradhan[2,3]**

[1] Department of Geography, University of Gour Banga, Malda, West Bengal 732103, India

[2] Centre for Advanced Modelling and Geospatial Information Systems (CAMGIS), School of Civil and Environmental Engineering, Faculty of Engineering & IT, University of Technology Sydney, Ultimo, NSW 2007, Australia

[3] Earth Observation Center, Institute of Climate Change, Universiti Kebangsaan Malaysia, UKM, 43600 Bangi, Selangor, Malaysia